DOE/EI/11292--18

MASTER

Thermo Electron
CORPORATION

DISCLAIMER

Thermo Electron
CORPORATION

Report No. TE4258-247-81

DOE
ADVANCED THERMIONIC
TECHNOLOGY PROGRAM

PROGRESS REPORT NO. 46

January, February, March
1981

DOE Contract DE-AC02-81ET11291

Prepared by

Thermo Electron Corporation
101 First Avenue
Waltham, Massachusetts 02254

Blank Page

TABLE OF CONTENTS

INTRODUCTION AND SUMMARY

The advanced Thermionic Technology Program at Thermo Electron Corporation is sponsored by the Department of Energy (DOE). The primary long-term goal is to improve thermionic performance to the level that thermionic topping of fossil-fuel powerplants becomes technically possible and economically attractive. An intermediate goal is to operate a thermionic module in a powerplant during the mid-1980's. A short-term goal is to demonstrate reliable thermionic operation in a combustion environment.

This report covers progress made during the three-month period from January through March 1981. During this period, significant accomplishments include:

- Continuing stable output from the combustion test of the one-inch diameter hemispherical silicon carbide diode (Converter No. 239) at an emitter temperature of 1730 K for a period of over 6400 hours.
- Demonstration of an additive oxygen effect in a research diode (Converter No. 258) with a cesium-graphite reservoir located in the collector.
- Preliminary testing of the four-diode module.
- Evaluation of a research diode (Converter No. 261) with ZrO_2-Mo cermet electrodes.

DOE CONTRACT NO. DE-AC02-81ET11292
WORK BREAKDOWN STRUCTURE

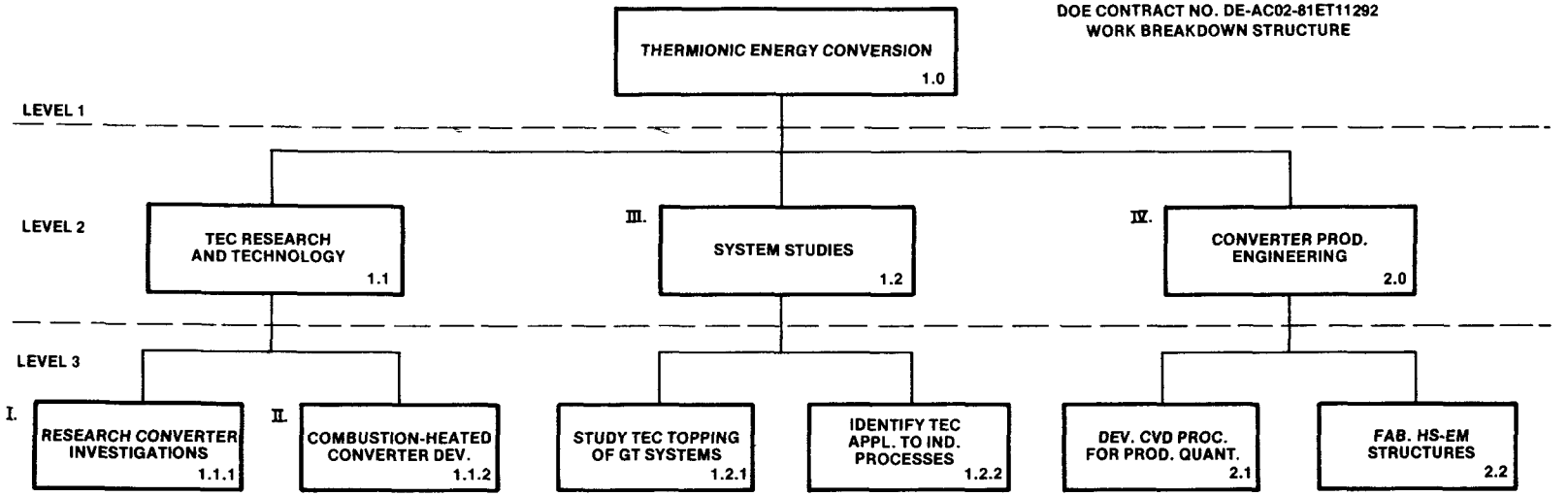

NOTE: ROMAN NUMERALS DESIGNATE LEVEL AT WHICH TASKS ARE TO BE REPORTED

I. RESEARCH CONVERTER INVESTIGATIONS

The objective of this task is to investigate electrode pair performance as it varies with emitter and collector composition, microstructure and additives using variable-spaced research converters heated by electron bombardment. Converter characteristics will be measured as a function of emitter temperature, collector temperature, cesium pressure, interelectrode spacing and, if applicable, additive gas pressure

A. Investigations of the W(100)-O-Zr-C Electrode

In the last quarterly report, three methods of dosing a W(100) crystal with zirconium and carbon monoxide (CO) were discussed. A minimum work function of 2.3 eV was obtained. During this reporting period, a fourth dosing technique was investigated.

The fourth method of exposing W(100) to zirconium and CO is simultaneous deposition. The cleaned W(100) at room temperature is first exposed to 120 L CO, followed by deposition of zirconium in the presence of either 1×10^{-7} or 5×10^{-7} torr CO for 16 to 18 minutes. The zirconium flux onto the crystal is estimated to be 4×10^{12} atoms/cm^2-sec. The work function after a 1700 K vacuum anneal for 3 minutes was

2.39 to 2.44 eV, which is only 0.1 eV higher than the minimum obtained for the alternate doses in the third method. This fourth method has the advantage that monitoring of the Zr/W ratio is not required. To within $\pm$ 0.005 eV, the final work function is independent of whether the CO pressure is 1×10^{-7} or 5×10^{-7} torr.

A summary of the four dosing methods and the minimum work function obtainable by each method is listed in Table I. The W(100) crystal is cleaned before each dosing method by flashing it to 2400 K for 10 to 20 seconds. Work functions below 2.4 eV can be obtained by any of the last three dosing methods.

The Zr/W, O/W and C/W ratios for various low work function surfaces are shown in Table II, along with the initial method of dosing. The data appear to fit into two distinct categories, denoted "high-carbon" case and "low-carbon" case. The C/W ratio for the low-carbon case is less than one-half of the corresponding ratio for the high-carbon case and the Zr/W ratio is also lower for the low-carbon case.

The stability of the 2.3 to 2.4 eV work function surface was investigated by exposing the crystal to ambient background for 1 to 2 days and by heating the crystal at high temperatures (see Table III). The simultaneous dosing technique (i.e., Method 4) appears to produce a more stable surface under background adsorption than Method 3.

TABLE I

CORRELATION OF DOSING METHOD WITH MINIMUM WORK FUNCTION

DOSING METHOD NO.	MINIMUM WORK FUNCTION (eV)	DOSING METHOD		VACUUM ANNEAL
		FIRST EXPOSURE, T	SECOND EXPOSURE, T	
1	2.53	Zr, 300 K	CO, 1500 K	1600 - 1700 K
2	2.38	CO, 1200 K	Zr, 300 K	1200 - 1800 K
3	2.29	CO, 300 K	Zr, 300 K	1700 K
4	2.39	CO, 300 K	Zr+CO, 300 K	1700 K

TABLE II

ATOMIC RATIOS FOR VARIOUS LOW WORK FUNCTION SURFACES

INITIAL DOSING METHOD NO.	WORK FUNCTION	Zr/W	O/W	C/W
3	2.29	1.01	3.86	1.45
3	2.29	1.03	3.65	1.55
3	2.34	1.15	3.28	1.65
3	2.38	1.13	4.75	1.63
4	2.39	1.06	4.68	1.82
4	2.39	1.07	4.84	1.56
Average (High-Carbon)	2.35 $\pm$ 0.04	1.08 $\pm$ 0.05	4.18 $\pm$ 0.66	1.61 $\pm$ 0.11
4	2.34	0.76	3.74	0.67
2	2.38	0.78	3.35	0.80
Average (Low-Carbon)	2.36 $\pm$ 0.02	0.77 $\pm$ 0.01	3.55 $\pm$ 0.20	0.74 $\pm$ 0.07

TABLE III

STABILITY OF W(100)-O-Zr-C SURFACES

DOSING METHOD NO.	WORK FUNCTION BEFORE TREATMENT	TREATMENT	WORK FUNCTION CHANGE AFTER TREATMENT	PERCENT OF ORIGINAL REMAINING AFTER TREATMENT		
				Zr/W	O/W	C/W
3	2.29	Bkgnd,1700 K,10 sec	+ 0.25	67	70	35
3	2.29	Bkgnd,1700 K,1 min	+ 0.21	69	84	39
4	2.39	Bkgnd,1700 K,1 min	- 0.05	71	77	43
3	2.34	1200 K, 60 min	+ 1.38	92	173	79
4	2.39	1300 K, 5 min 1500 K, 5 min 1700 K, 1 min	0.00	101	103	86
3	2.49	1700 K, 4 min	+ 0.13	89	90	71
3	2.50	1700 K, 30 min	+ 0.19	50	56	0
2	2.38	1800 K, 1 min	+ 0.67	78	48	11

The third entry in Table III corresponds to a conversion from the high-carbon to the low-carbon case, indicating that the two cases are closely related. Stability after a 1500 K heating for 5 minutes is obtained after the simultaneous dosing method. Longer heatings at 1700 K or shorter heatings at 1800 K cause depletion of the carbon concentration. It may be possible to restore the carbon concentration by providing slow carbon diffusion from the bulk or by heating the emitter in a small partial pressure of a carbon-containing gas.

In the last quarterly report, the minimum work function, after the zirconium and CO adsorption on W(100), occurred for a minimum tungsten concentration. This indicated that replacement of the W(100) substrate by a zirconium substrate might also produce a low work function. A zirconium foil was inserted into the surface characterization chamber, and cleaned by heating to 1800 K for one minute. The foil held at 1200 K was then exposed to 1.3×10^{-3} Pa (1×10^{-5} torr) CO for 400 minutes. Subsequent vacuum anneals from 1200 to 1800 K produced surfaces with work functions varying from 3.67 to 3.89 eV, much higher than the 2.3 to 2.5 eV work functions observed for zirconium and CO on W(100). Thus the W(100) substrate does play a definite role in the production of the low work function.

During the zirconium foil studies it was noticed that the zirconium Auger peaks changed markedly depending on the amount of carbon and oxygen contamination. A communication describing the details of this spectrum change has been submitted to the Journal of Vacuum Science and Technology.

B. Auger Analyses of ZrO_2-Mo Cermet Electrodes

Preoperational Auger analyses were performed on two nickel collectors and two tungsten emitters which had been plasma sprayed with a ZrO_2-Mo mixture by R. Henne of DFVLR. The coating thicknesses and weight percents of ZrO_2 and Mo as given by Henne are listed in Table IV.

The elemental atomic percent concentrations as determined by Auger analysis for the ZrO_2-Mo emitters and collectors are given in Table V. The subscript on the element abbreviation is the Auger peak energy used to calculate the percent concentrations. Sputtering time was 20 minutes for the collectors and 40 minutes for the emitters. The argon pressure was 5×10^{-5} torr and the ion energy was 2 kV. A relatively small amount of methane was present in the sputtering gas, which may account for part of the carbon signal after sputtering.

TABLE IV

LOW PRESSURE PLASMA ARC SPRAYED SPECIMENS

ELECTRODE	NO.	SUBSTRATE	COATING THICKNESS (μm)	BY WEIGHT (%)	
				ZrO_2	Mo
Collector	1	Nickel	90	20	80
Collector	2	Nickel	100	20	80
Emitter	1	Tungsten	20	50	50
Emitter	2	Tungsten	25	50	50

TABLE V

AUGER PERCENT CONCENTRATIONS FOR ZrO_2-Mo EMITTERS AND COLLECTORS

ELEMENT	AS ADMITTED				AFTER SPUTTERING			
	COLLECTORS		EMITTERS		COLLECTORS		EMITTERS	
	No. 1	No. 2	No. 1	No. 2	No. 1	No. 2	No. 1	No. 1
Mo_{2044}	32.7	24.9	27.4	33.0	54.1	38.4	39.6	33.2
Zr_{1845}	-	-	-	-	4.9	7.7	10.1	9.2
O_{510}	24.1	25.1	14.5	18.5	17.9	25.3	20.3	23.2
C_{273}	29.5	30.9	47.2	39.8	17.9	17.3	22.9	24.6
N_{380}	1.5	1.4	2.7	1.8	2.0	1.5	1.5	3.1
Ca_{291}	4.9	2.8	0.9	1.3	0.9	3.2	1.9	1.7
Si_{1620}	6.8	10.2	5.7	4.5	2.0	5.3	2.8	4.0
Na_{996}	-	1.8	1.6	1.2	-	0.3	-	0.5
Ni_{848}	-	-	-	-	-	0.5	0.7	0.4
Fe_{703}	-	-	-	-	-	0.4	-	-
Cl_{181}	0.5	2.8	-	-	-	-	-	-

The primary conclusion is that molybdenum is present in much higher concentrations than zirconium for both collectors and emitters. Additionally, small amounts of impurities such as nitrogen, calcium, silicon, sodium, nickel and iron are apparently deposited on the substrates in the plasma spray process since these impurities are present even after extended sputtering.

C. Postoperational Diagnostics

Postoperational diagnoses were performed for Converter No. 257 (Mo emitter, Mo_xO_y collector) and Converter No. 249 (electroetched CVD tungsten emitter, Mo_xO_y collector) to attempt to explain their different performances.

Converter No. 257 exhibited a high barrier index with resistive I-V characteristics, while Converter No. 249 gave a low barrier index of 2.06 eV. The oxygen concentrations of the collectors were comparable: 12,300 ppm for Converter No. 257 and 9880 ppm for Converter No. 249.

After operation, the collector of Converter No. 257 was uniformly dark grey while the collector of Converter No. 249 was patchy grey with a black ring near the outer edge. Auger elemental concentrations for the as admitted

electrodes are given in Table VI. The letters A, B and C refer to grey areas of Collector No. 249, while D refers to a point on the outer black edge. The following results can be noted:

1) The surfaces are free of unusual contaminants except for silicon on Emitter No. 257.

2) Emitter No. 249 shows no molybdenum, indicating oxygen transport to the emitter does not occur via a molybdenum oxide.

3) Some tungsten is present on Collector No. 249, predominantly in the grey areas. In an oxygenated converter, tungsten oxides formed on the emitter can apparently vaporize and deposit onto the collector. This tungsten on the collector evidently does not degrade the converter's performance.

4) Both collectors are essentially free of carbon. The explanation of this rather unusual finding will be given later.

The collectors of Converter Nos. 257 and 249 were sputtered with 2 kV argon ions (see Figures 1 and 2). High concentrations of cesium and low concentrations of carbon were found even after extended sputtering of both converters. Molybdenum, cesium and oxygen were present after sputtering, in concentrations from 23 to 38 percent for both collectors.

TABLE VI

POSTOPERATIONAL AUGER ANALYSES OF CONVERTER NOS. 249 and 257

	CONVERTER NO. 257		CONVERTER NO. 249				
	EMITTER (Mo)	COLLECTOR (Mo_xO_y)	EMITTER (Electroetched W CVD)	COLLECTOR (Mo_xO_y)			
				A	B	C	D
Mo	40.9	21.7	-	11.3	9.9	9.4	15.2
W	-	-	38.3	9.9	12.0	11.4	2.7
Cs	16.4	45.9	32.6	42.4	41.1	40.9	45.8
C	18.9	1.1	8.4	1.2	1.6	1.9	1.4
O	14.1	31.2	20.7	35.2	35.4	36.4	34.9
Si	9.6	-	-	-	-	-	-

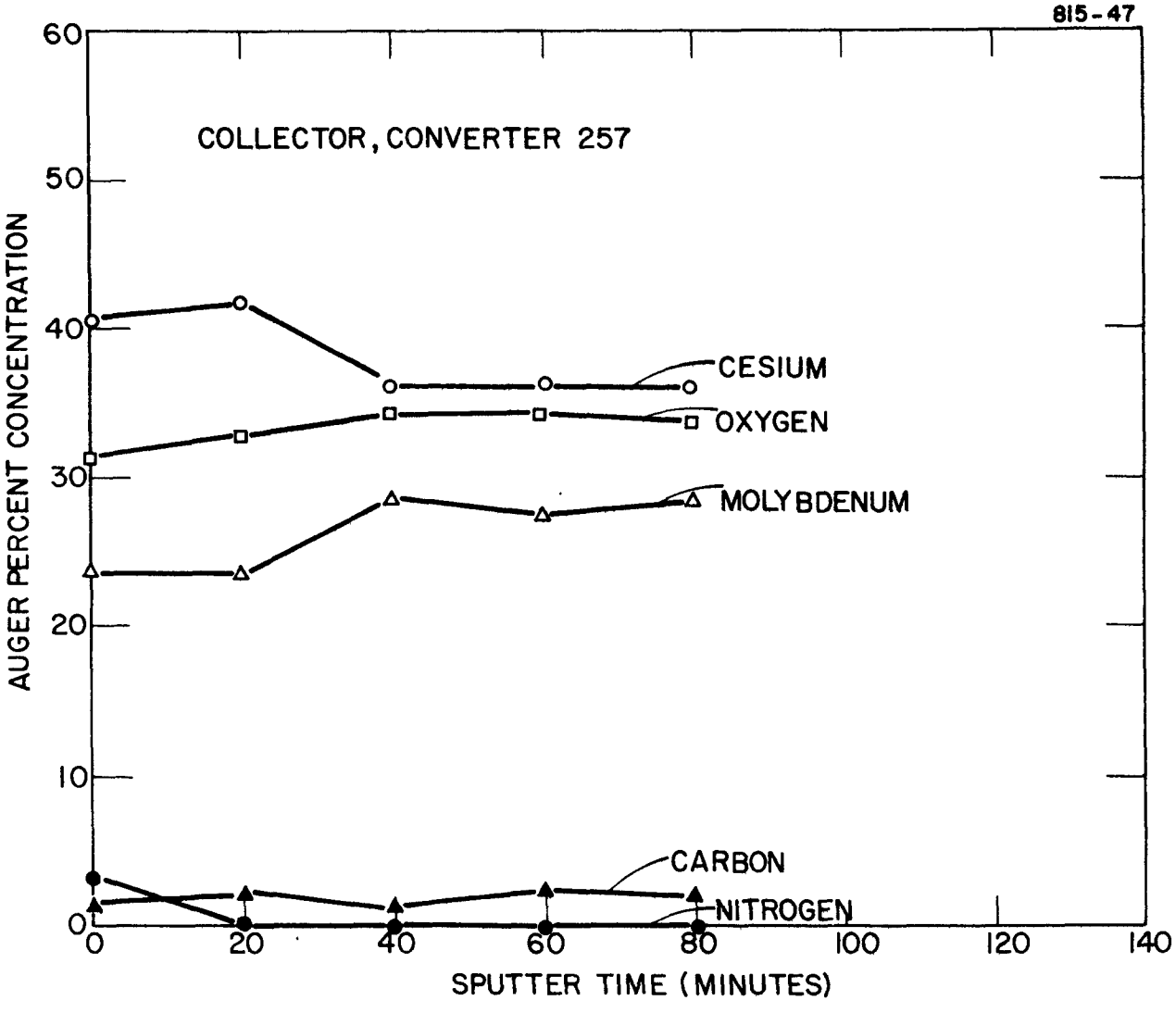

Figure 1. Auger Concentration Versus Sputter Time for the Collector of Converter No. 257

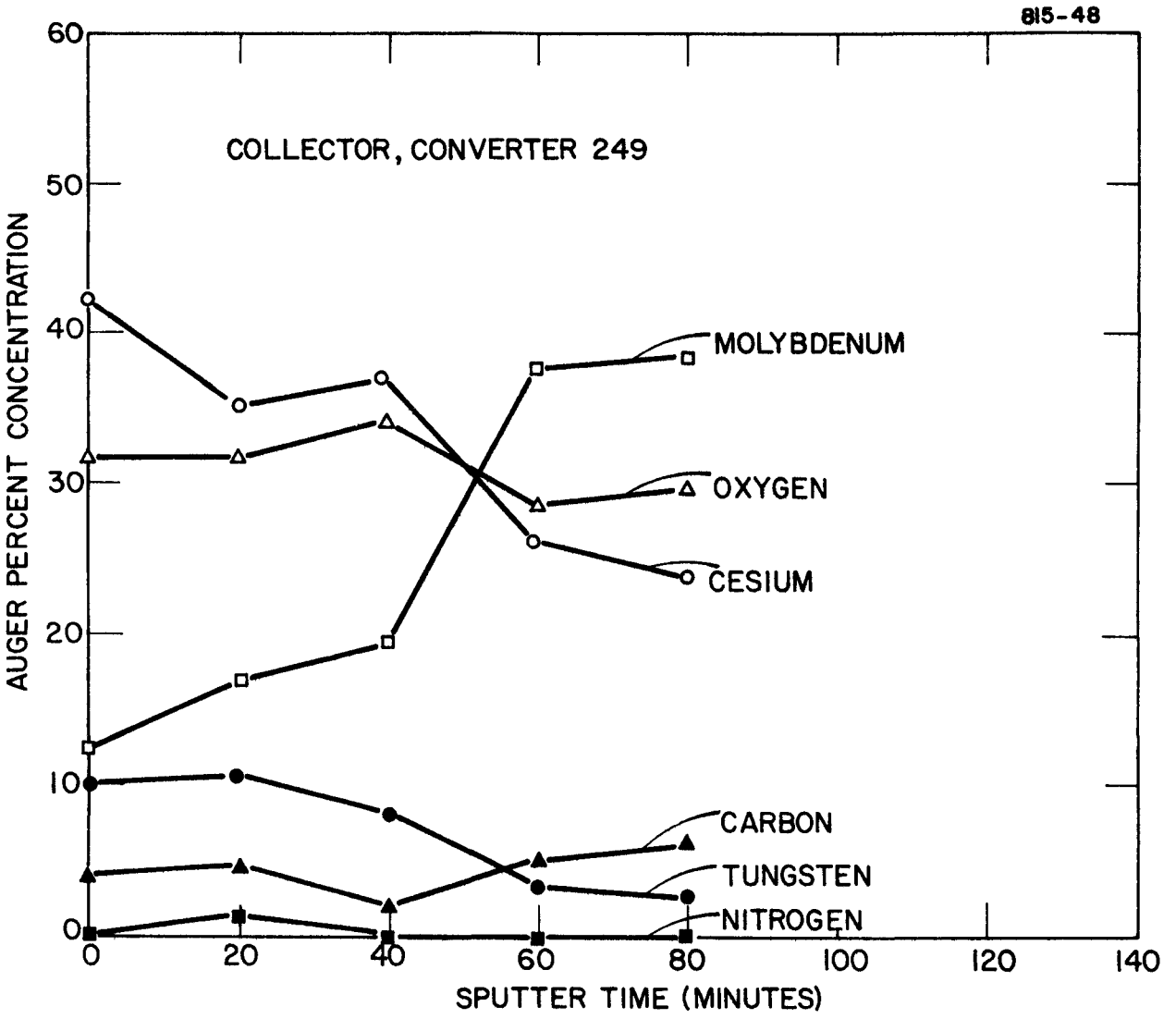

Figure 2. Auger Concentration Versus Sputter Time for the Collector of Converter No. 249

For comparison purposes, a piece of as deposited molybdenum oxide (V-66 A, 12,700 ppm oxygen) was also sputtered in the surface characterization chamber (see Figure 3). Large amounts of carbon are present even after sputtering. This carbon can be removed easily by heating the sample to 1100 K for 30 minutes in ultrahigh vacuum. This suggests that bulk carbon combines with oxygen to form carbon monoxide which desorbs leaving a carbon-free surface. This result agrees with the observation that essentially no carbon is found on the collectors of Converter Nos. 257 and 249.

The oxide layers of Collector Nos. 257 and 249 were machined to a depth of 4 mils. Cesium was present in large amounts (35 to 46%) at this depth, confirming that cesium diffuses deep into the molybdenum oxide layer during converter operation.

The primary conclusions from the postoperational analyses of Converter Nos. 257 and 249 are:

1. No obvious differences exist in elemental concentrations for the two converters, which would explain their performance discrepancies.
2. Cesium penetrates deep into molybdenum oxide layers during converter operation.
3. Carbon can be removed from molybdenum oxide layers simply by mild heating in vacuum.

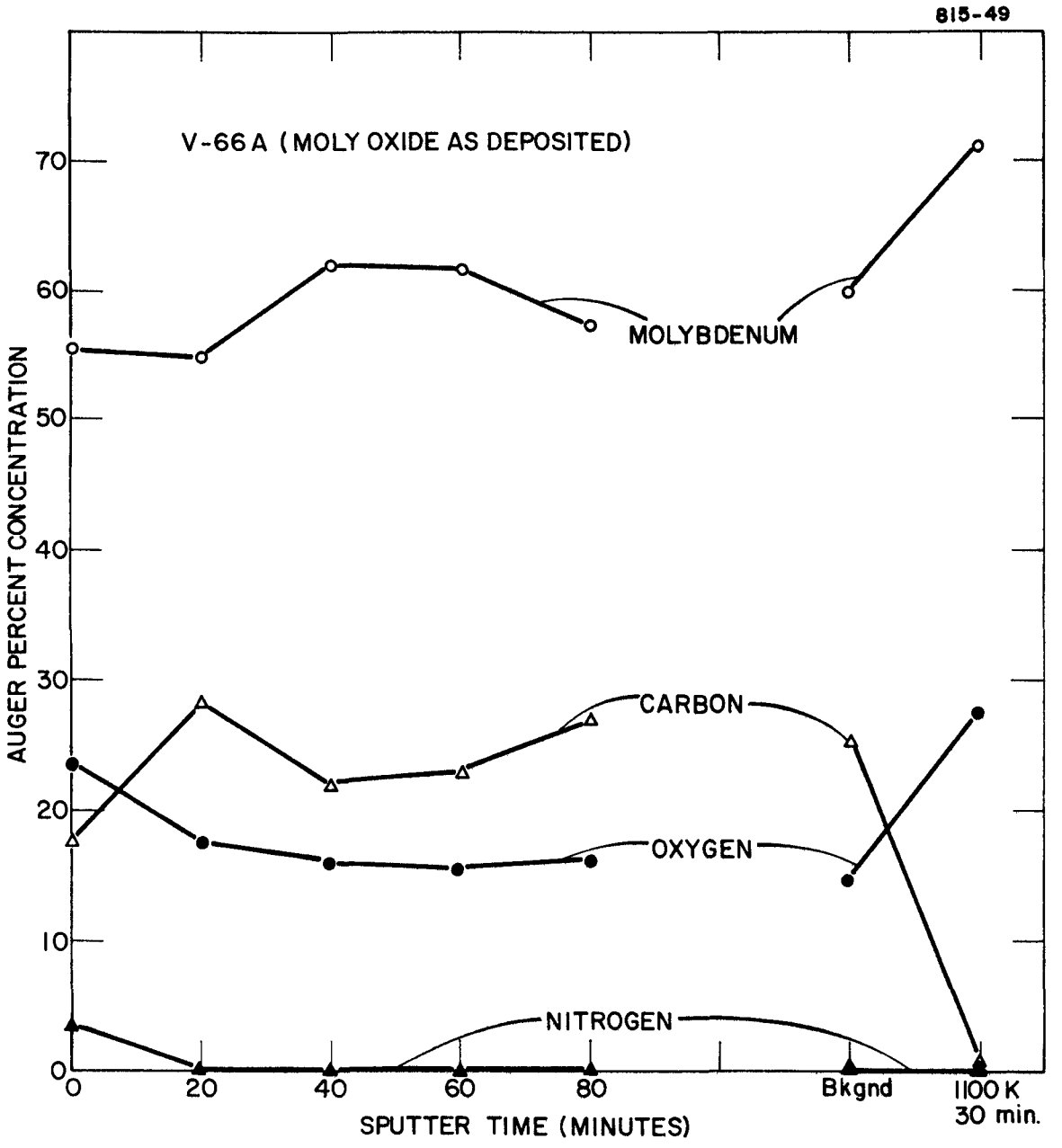

Figure 3. Auger Concentration Versus Sputter Time for Molybdenum Oxide Deposit V-66A

D. Converter No. 246: Tungsten Emitter, Nickel Collector, Heat Flux Diode

During this reporting period, the heat flux diode output was characterized at an emitter temperature of 1700 K. A typical cesium reservoir temperature family at T_E = 1700 K, T_C = 850 K and d = 0.25 mm is given in Figure 4. The optimized performance at T_E = 1700 K and various interelectrode spacings is shown in Figure 5. The barrier index is 2.06 eV at 5 A/cm^2.

Additional collector work function measurements were made during this reporting period. A retarding plot measurement made at an emitter temperature of 1300 K and a collector temperature of 600 K gave a minimum value of 1.74 eV. This value is two tenths of an electron volt higher than that previously reported.[1] This recent determination does not appear to be consistent with the barrier index of 2.06 eV.

E. Converter No. 261: ZrO_2-Mo Cermet Electrodes

Converter No. 261 contains ZrO_2-Mo cermet electrodes. The electrodes were plasma sprayed at Deutsche Forschungs-und Versuchsanstalt fur Luft-und Raumfart (DFVLR) in Stuttgart, Germany. The technique used to form the coatings is described in References 2 and 3.

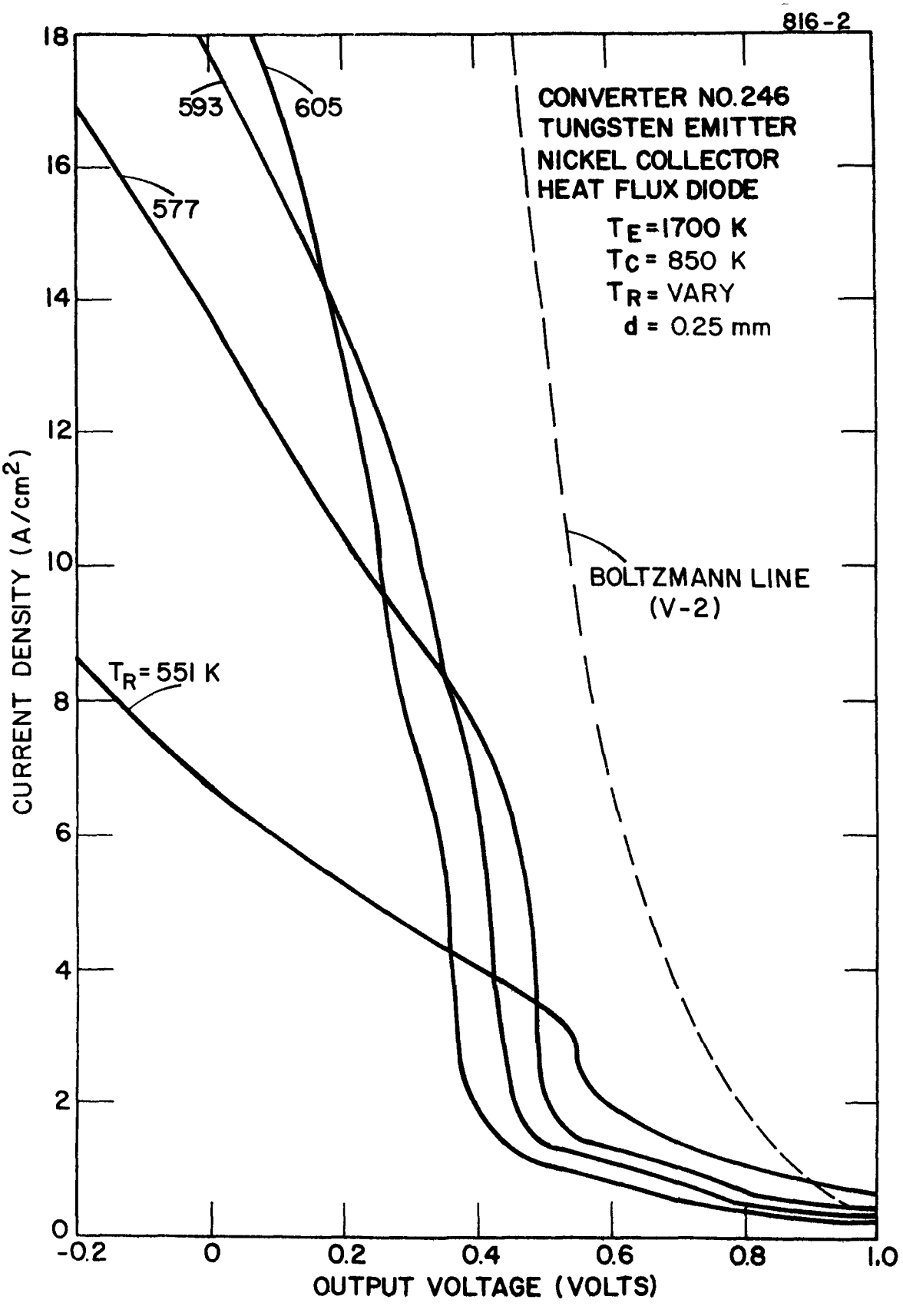

Figure 4. Cesium Reservoir Temperature Family at T_E = 1700 K, T_C = 850 K and d = 0.25 mm for Converter No. 246

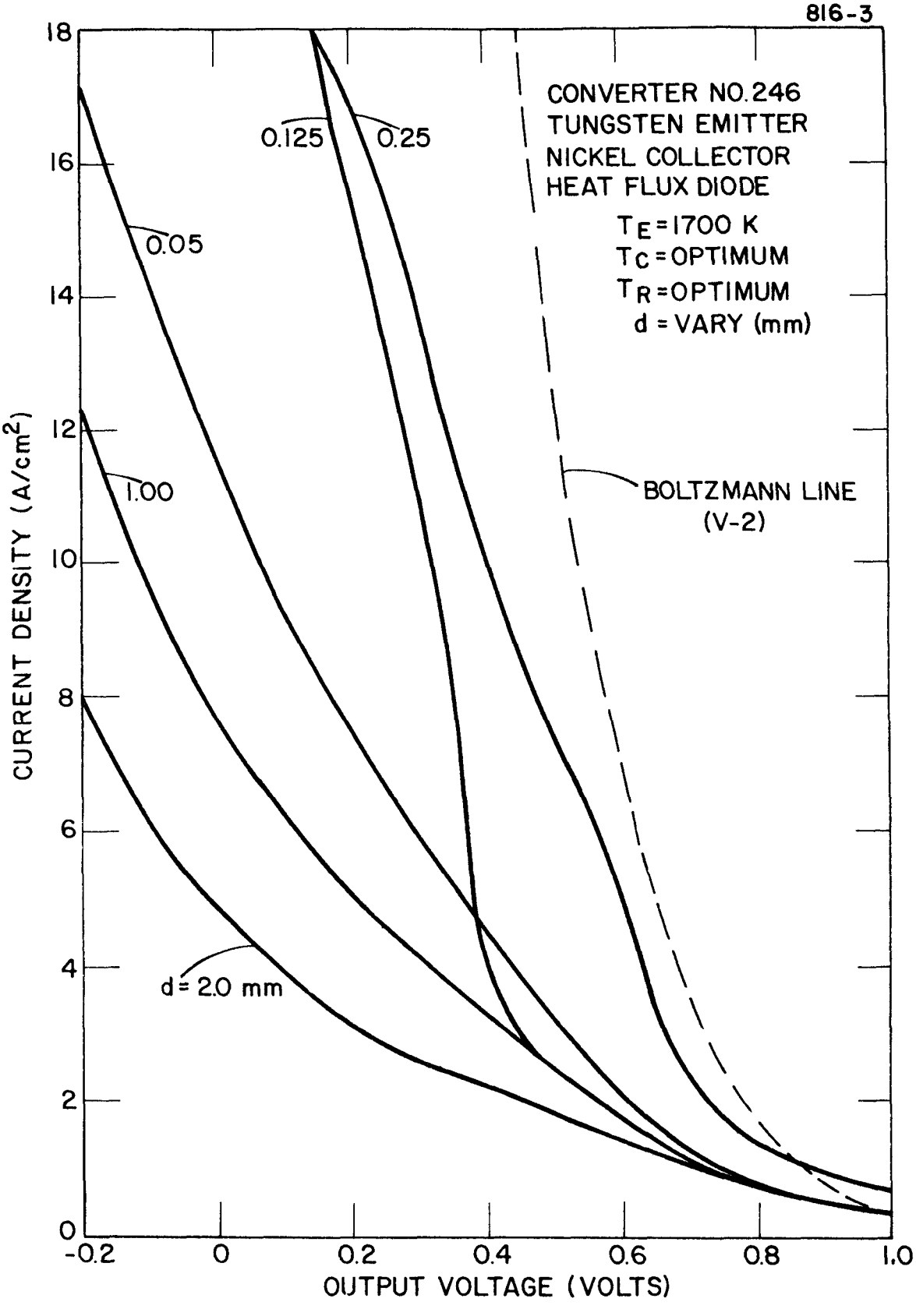

Figure 5. Optimized Converter Performance at T_E = 1700 K and Various Interelectrode Spacings for Converter No. 246

Two emitter-collector pairs were coated using the above technique. The particulars of the two electrode pairs are given in Table IV. The information contained in this table was provided by R. Henne of DFVLR. Upon receipt at Thermo Electron, a number of diagnoses were performed on the electrodes (cf. Section IB). Scanning Electron Micrographs (SEMs) of Emitter No. 1 and Collector No. 1 are shown in Figure 6.

Emitter No. 1 was paired with Collector No. 1 and assembled into a variable-spaced research converter. Current-voltage characteristics were obtained at emitter temperatures of 1700 and 1600 K as a function of collector temperatures, cesium pressures and inter-electrode spacings.

The initial output of the diode was quite erratic. Figures 7 and 8 show cesium reservoir temperature families at the identical conditions of T_E = 1700 K, T_C = 750 K, and d = 0.50 mm. The family of curves in Figure 8 was generated immediately following that of Figure 7. It was not possible to correlate changes in output with emitter or collector temperature excursions. Cesium families were not reproducible for the initial 25 hours of the diode's life.

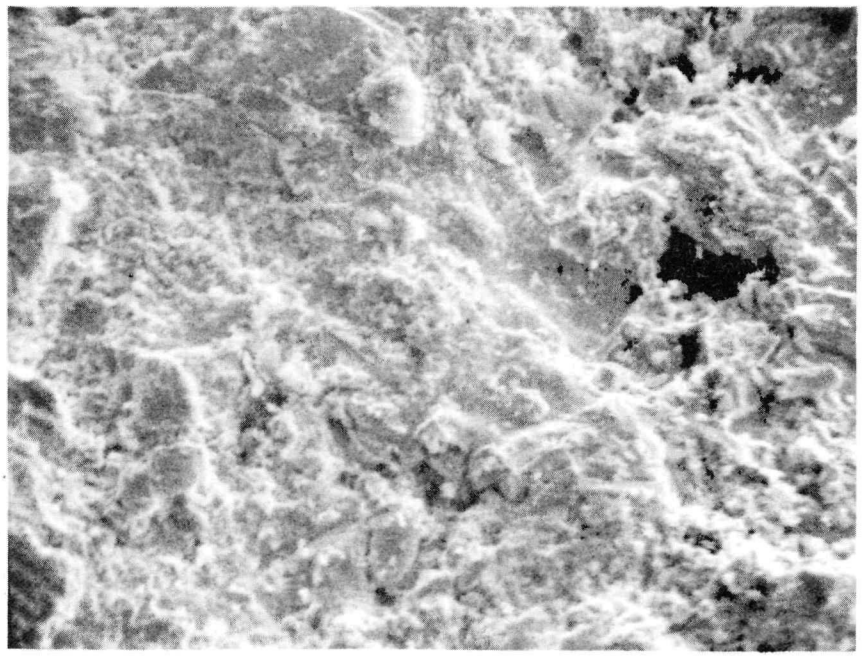

EMITTER NO. 1

COLLECTOR NO. 1

Figure 6. SEM's of ZrO_2-Mo Cermet Electrodes (1000 X)

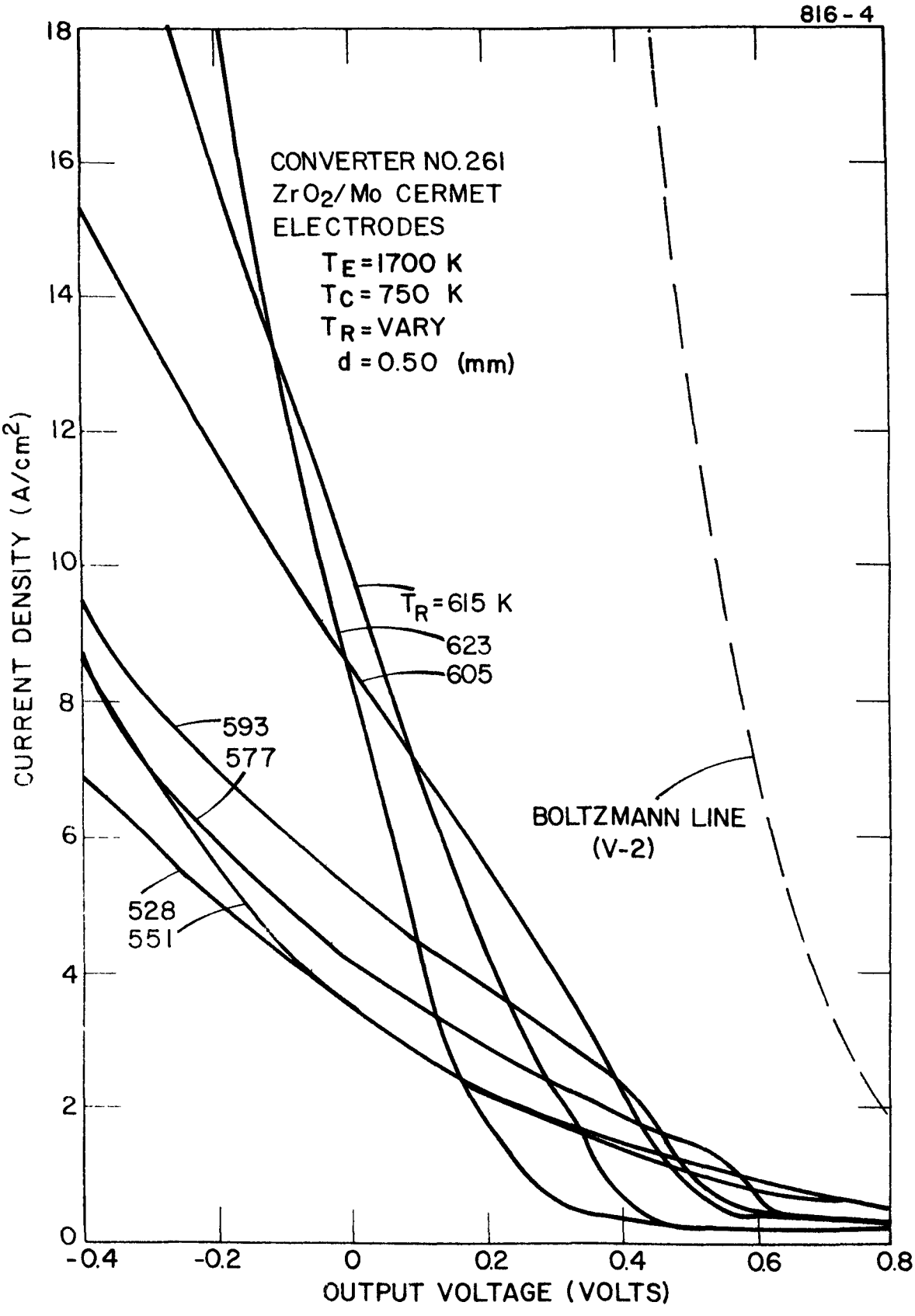

Figure 7. Cesium Reservoir Temperature Family at T_E = 1700 K, T_C = 750 K and d = 0.50 mm for Converter No. 261

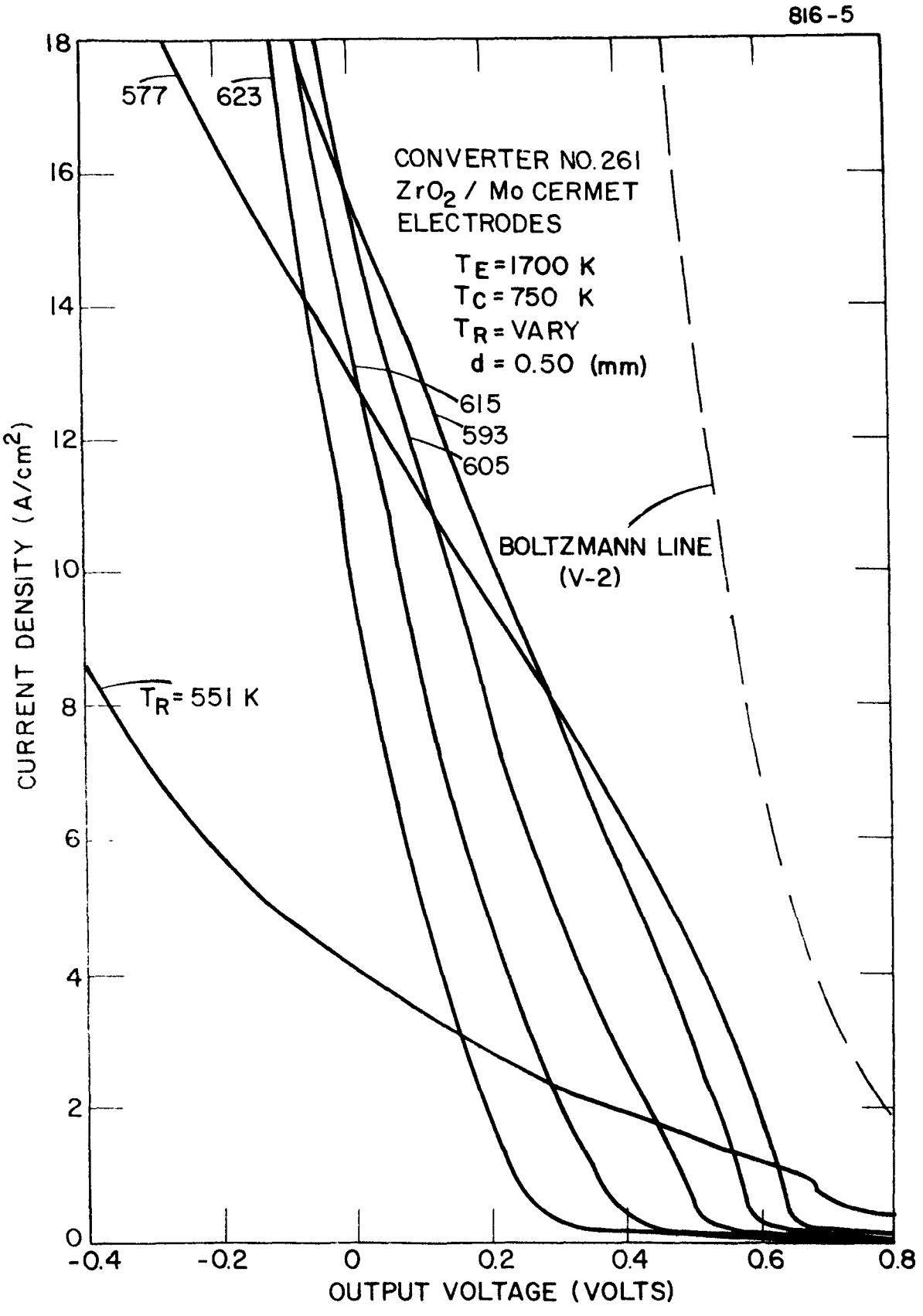

Figure 8. Cesium Reservoir Temperature Family at T_E = 1700 K, T_C = 750 K and d = 0.50 mm for Converter No. 261

After approximately 25 hours of operation, the output became more stable. A cesium reservoir temperature family at T_E = 1600 K, T_C = 800 K and d = 0.125 mm is given in Figure 9. The converter was optimized for collector temperature and cesium pressure at T_E = 1600 K. This result is given, parametric in interelectrode spacing, in Figure 10. At these conditions, the barrier index was 2.20 eV at 5 A/cm^2.

It should be noted that the electrodes were subjected to a high-temperature outgassing prior to assembly into the diode. The emitter and collector were held at 1725 and 1225 K, respectively, for one hour in an ultrahigh vacuum chamber at 3.5 x 10^{-7} torr. It is not known if this procedure adversely affected emitter and collector surface characteristics.

F. Converter No. 258: Tungsten Emitter, Nickel Collector, Integral Cesium-Graphite Reservoir

This converter contains two cesium reservoirs, a conventional liquid cesium reservoir and a graphite slug contained inside the collector. The collector assembly is shown in Figure 11. The graphite slug is in contact with the converter atmosphere via a small hole drilled into the collector body.

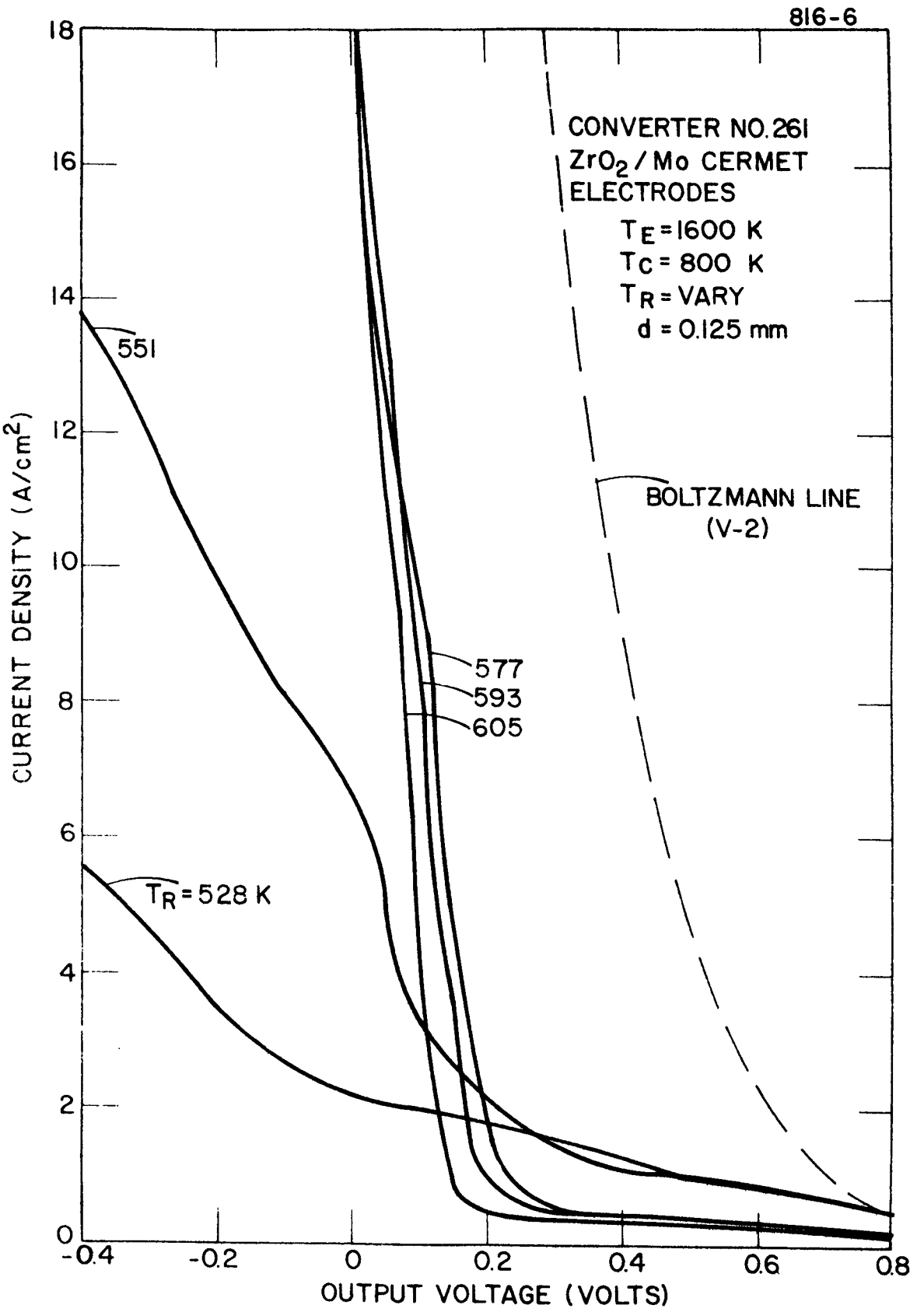

Figure 9. Cesium Reservoir Temperature Family at T_E = 1600 K, T_C = 800 K and d = 0.125 mm for Converter No. 261

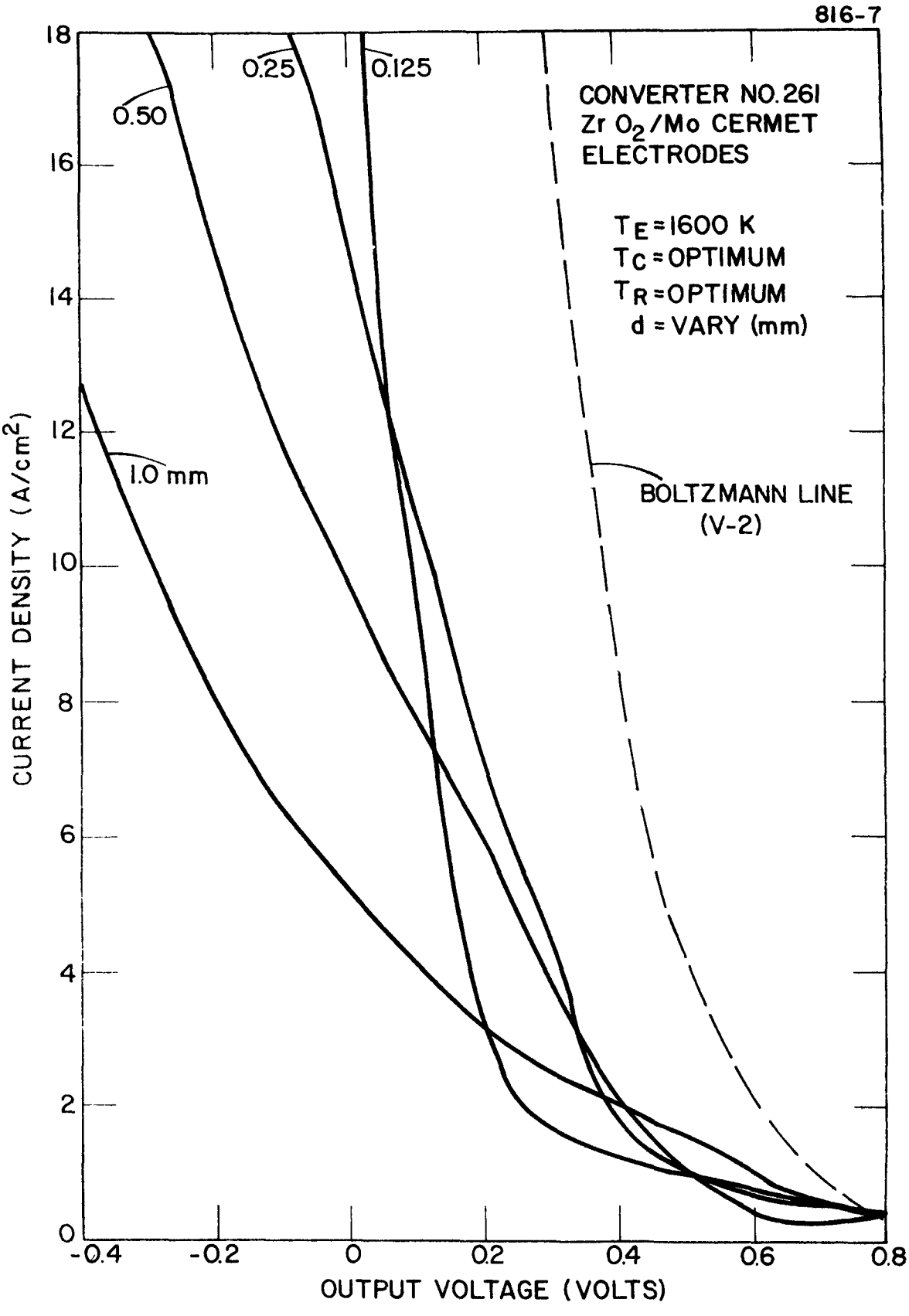

Figure 10. Optimized Converter Performance at Various Spacings for Converter No. 261

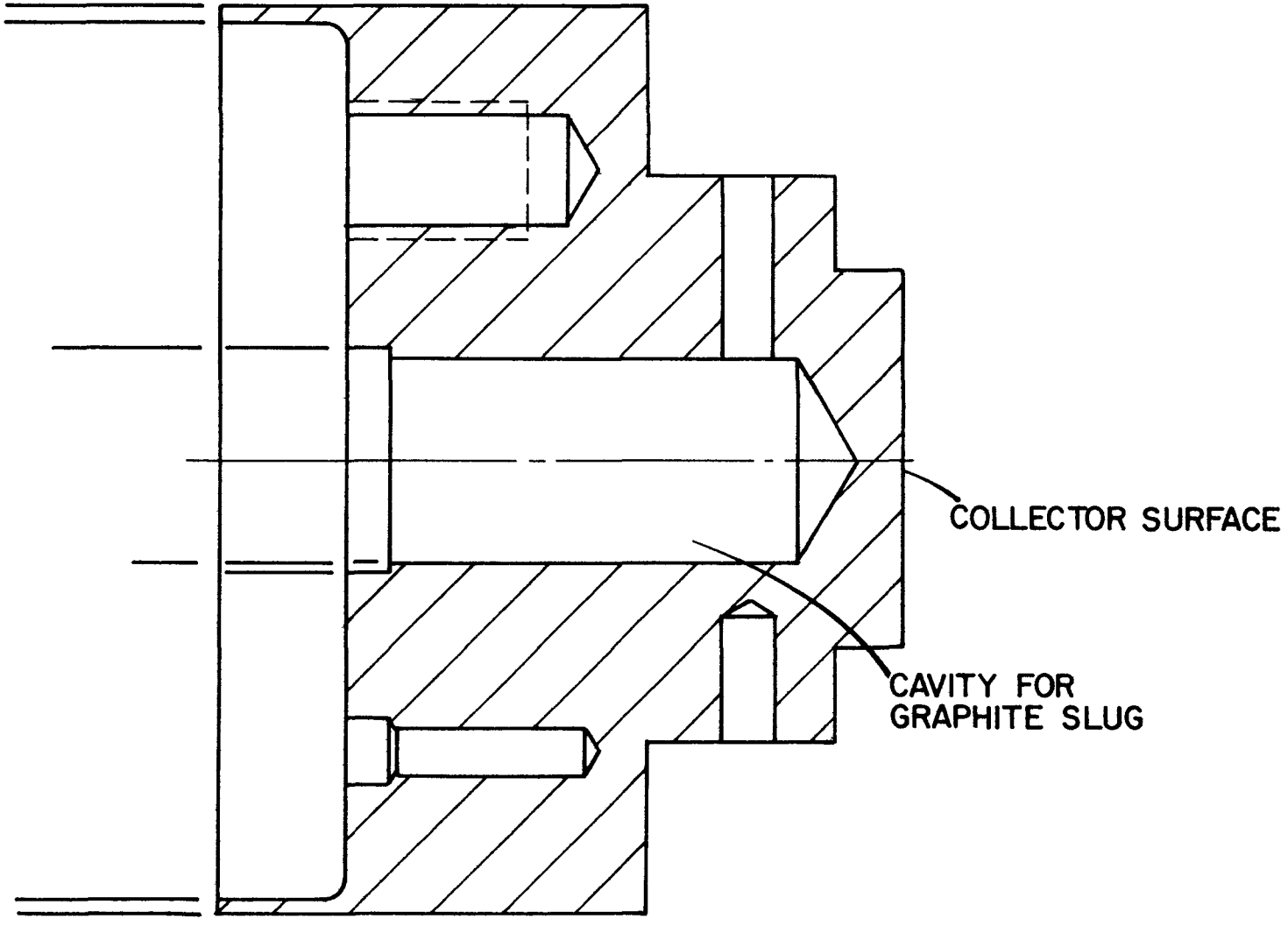

Figure 11. Collector with Internal Graphite-Cesium Reservoir

Converter output was mapped using the liquid cesium reservoir. Typical output characteristics as a function of liquid cesium temperature, T_R, at an emitter temperature of 1750 K are given in Figures 12 and 13. The barrier index was 2.22 eV at 5 A/cm^2.

The diode parameters for a minimum barrier index at an emitter temperature of 1750 K and a current density of 5 A/cm^2 were T_C = 850 K, T_R = 577 K (2 torr cesium) and d = 0.25 mm. Anticipating some cesium consumption the graphite was soaked in 2 torr cesium at a temperature of 820 K. After a period of 24 hours at these conditions, the converter was cooled and the excess cesium was pinched off. Approximately 0.1 gram of cesium had reacted with the graphite.

A collector family at T_E = 1750 K employing the cesium-graphite reservoir in the collector is given in Figure 14. The cesium pressure in the converter for a given cesium-graphite reservoir temperature was inferred by comparing the data in Figure 14 with liquid reservoir and collector temperature families taken prior to pinch off. The correlation of cesium pressure and collector temperature is given in Figure 15. The equivalent liquid cesium reservoir temperature is also shown in this figure.

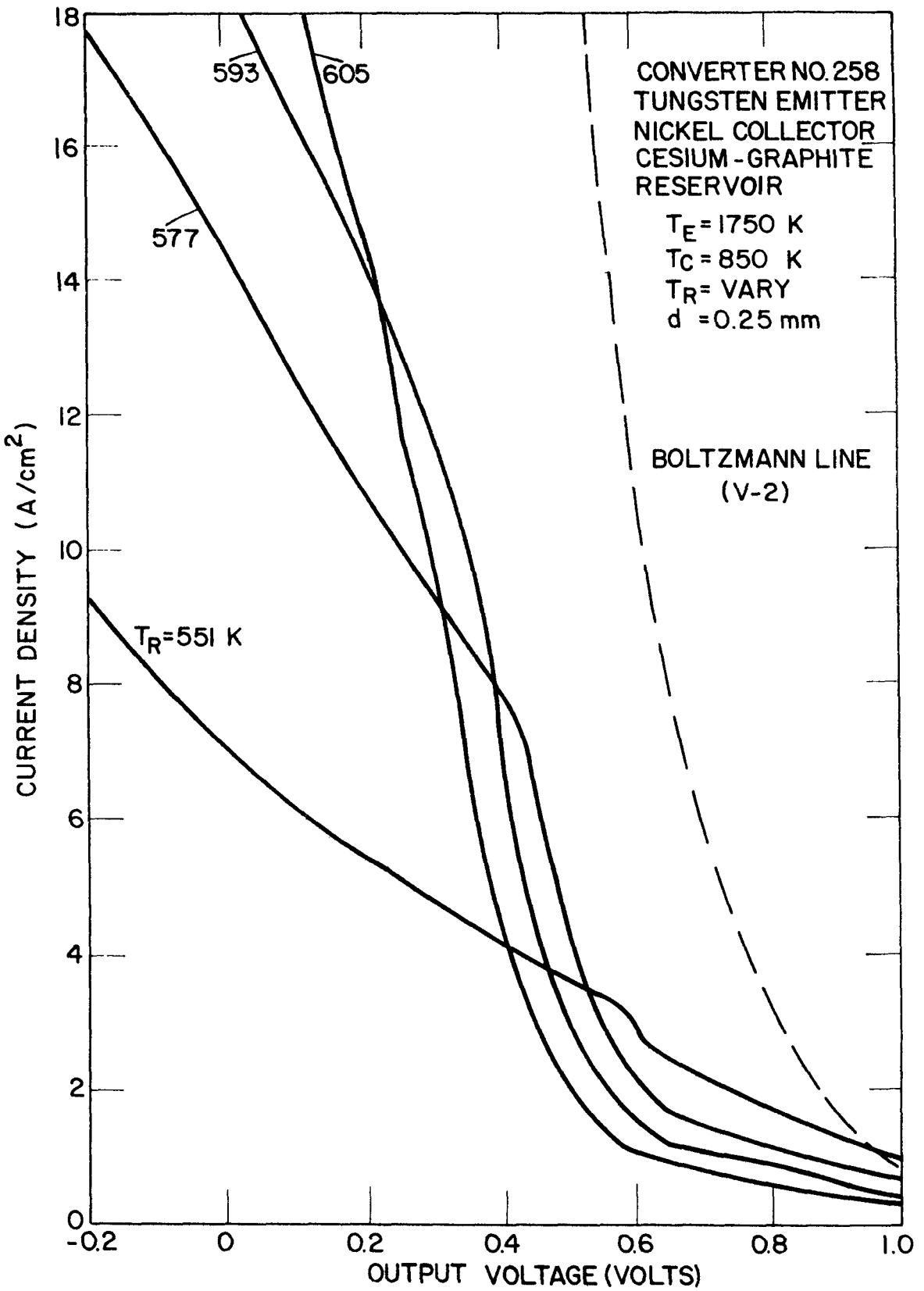

Figure 12. Cesium Reservoir Temperature Family at T_E = 1750 K, T_C = 850 K and d = 0.25 mm for Converter No. 258

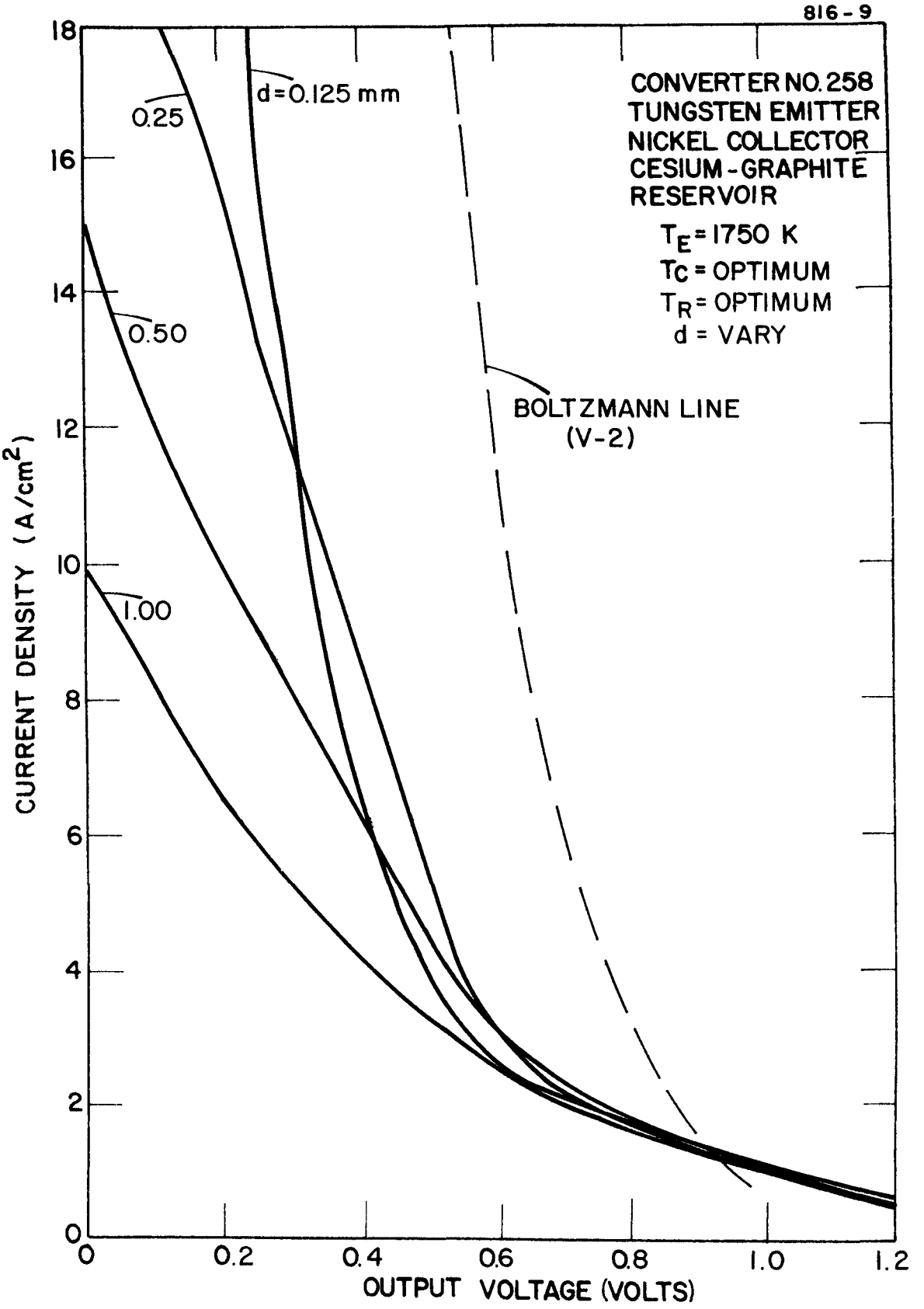

Figure 13. Optimized Converter Performance at T_E = 1750 K, and Various Interelectrode Spacings for Converter No. 258

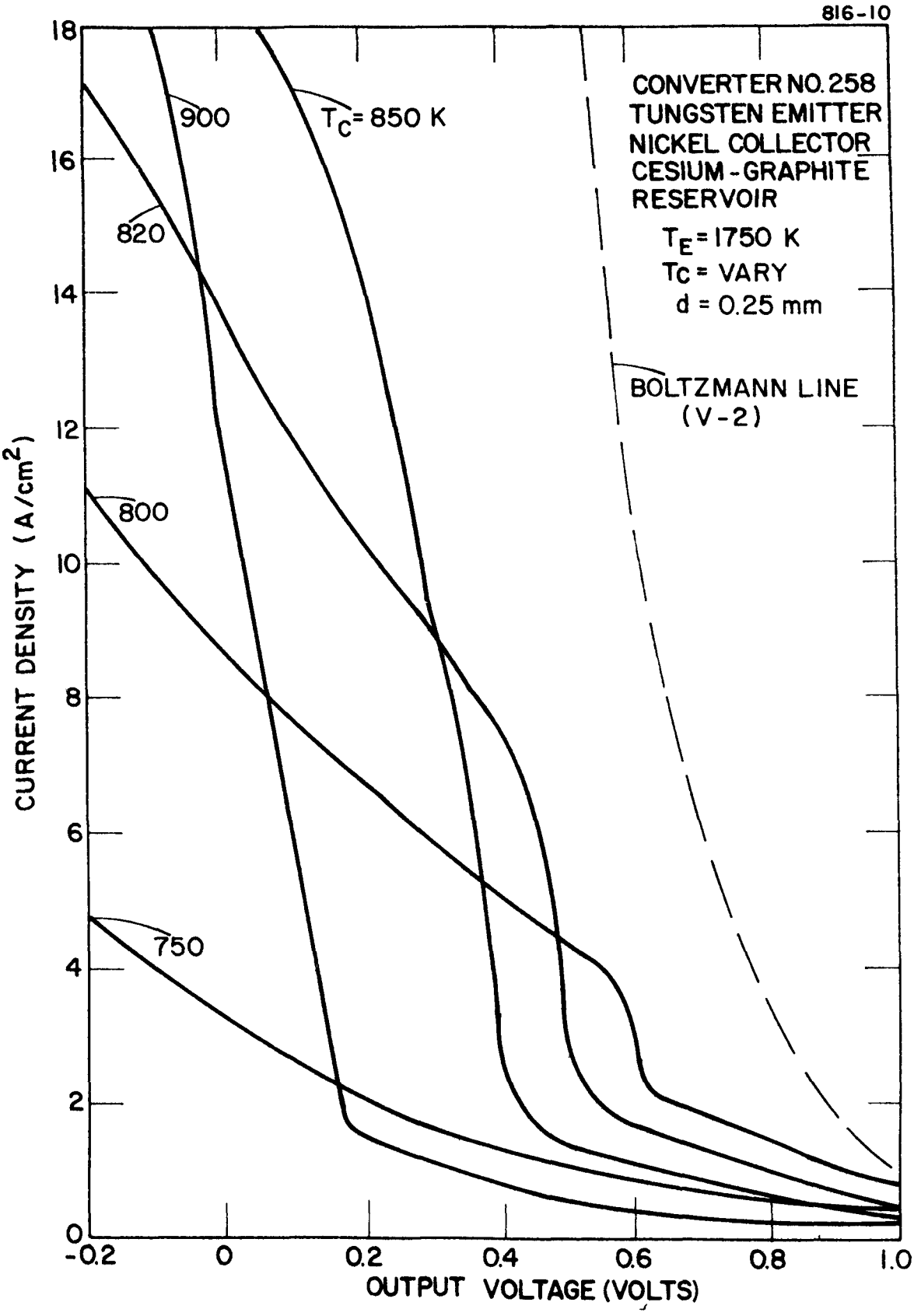

Figure 14. Collector Family at T_E = 1750 K, and d = 0.25 mm Using Cesium-Graphite Reservoir in Collector for Converter No. 258

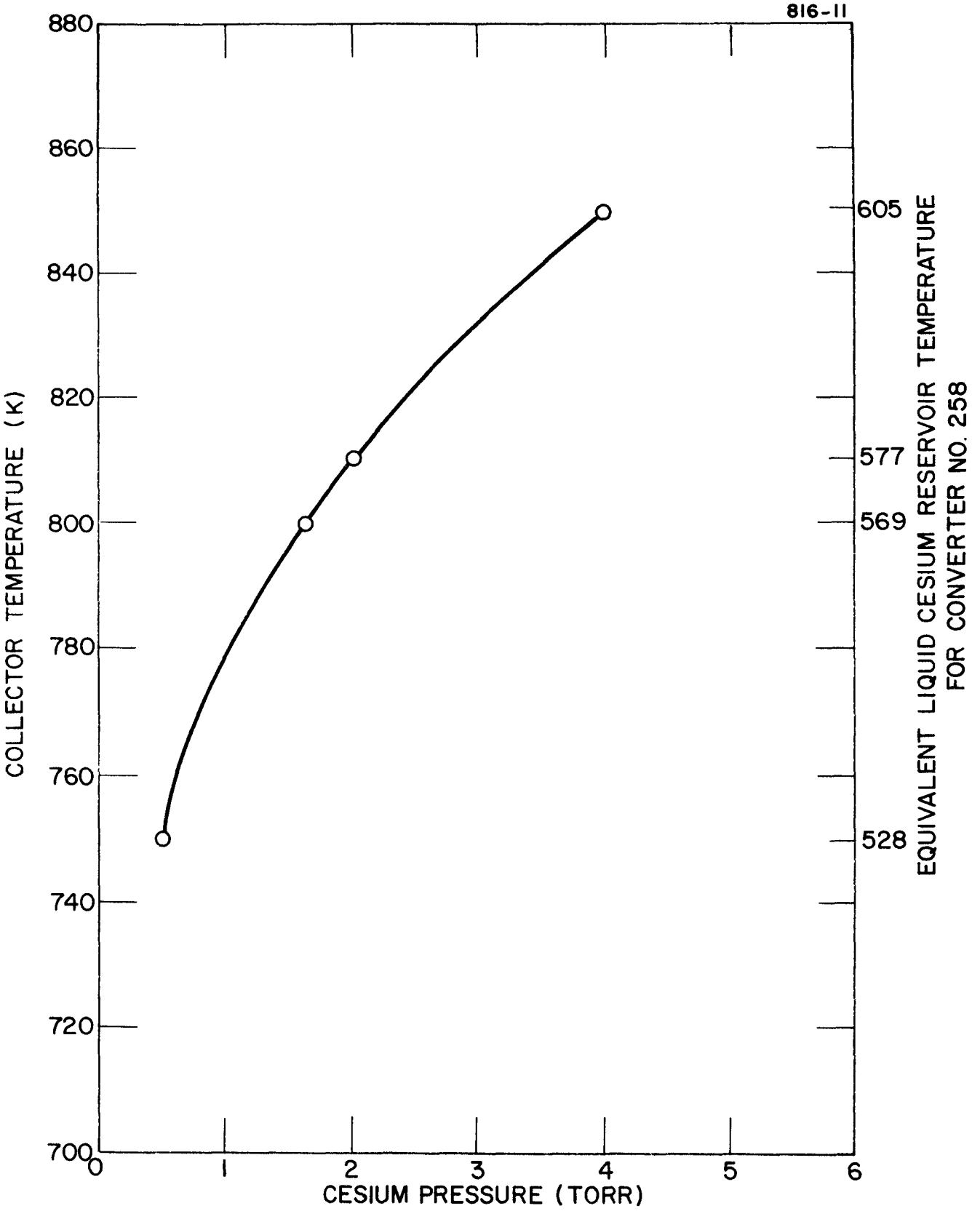

Figure 15. Cesium and Cesium-Graphite Reservoir Vapor Pressure Curve for Converter No. 258

For the first 250 hours of testing, the diode operated at T_E = 1750 K, T_C = 820 K and d = 0.25 mm with no change in output. Performance remained stable to room temperature through six thermal cycles and a number of collector temperature excursions to above its soak point.

After 250 hours of operation, a change in output was noticed. Emitter saturation current had increased and the collector work function had apparently increased. Figure 16 shows the output before and after the change. The curve taken on the 16th of February was typical of the output for the first 250 hours after the liquid reservoir pinch-off. For convenience, this output will be referred to as "Mode 1". The change to high emitter saturation current and high collector work function will be rreferred to as "Mode 2". Typically, the diode would begin operation after shutdown in Mode 1 and flip to Mode 2 after a period of 5 to 10 hours.

It is hypothesized that the diode is oxygenated in Mode 2. A number of observations support this interpretation:

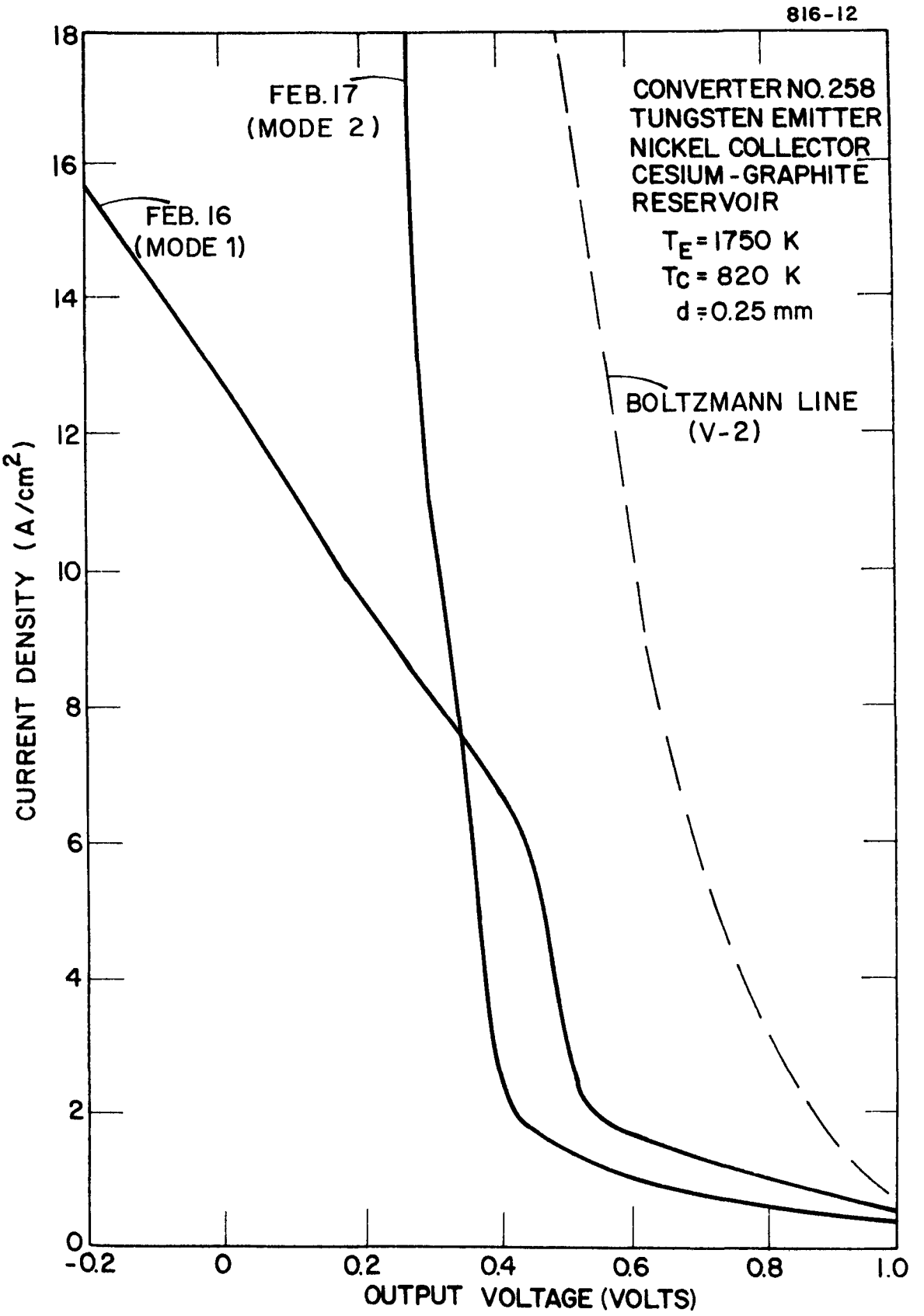

Figure 16. Current-Voltage Characteristics at T_E = 1750 K, T_C = 820 K and d = 0.25 mm Showing Two Modes of Operation for Converter No. 258

1. A liquid cesium reservoir was established in the diode by attaching a heater-cooler to the pinch-off. This reservoir was cooled slowly while monitoring diode output. A change in output signified that the liquid reservoir was pumping cesium. Using this method, it was determined that the cesium pressure during either mode was identical (i.e., 2 torr). Thus the cesium-graphite reservoir had indeed reestablished the cesium pressure at which it had been soaked.

2. At constant cesium pressure, the addition of a minute amount of oxygen would decrease the emitter work function, increasing emitter saturation current. This statement is based on the characteristics of many thermionic converters with oxide (either tungsten or molybdenum) collectors.

3. A collector temperature family taken in Mode 2 (given in Figure 17), shows the optimum collector temperature has shifted down to 775 K. This lower collector temperature and coinciding lower cesium pressure are typical of additive oxygen diodes.

If oxygen is responsible for the second mode of operation, one suspects that the graphite is its source. The collector temperature family in Figure 17 shows a growing output current with increasing collector temperature. However, it must be noted that changes in collector temperature also dictate changes in cesium pressure. The addition of beneficial amounts of oxygen via a cesium-graphite reservoir is an exciting possibility that had not been considered previously.

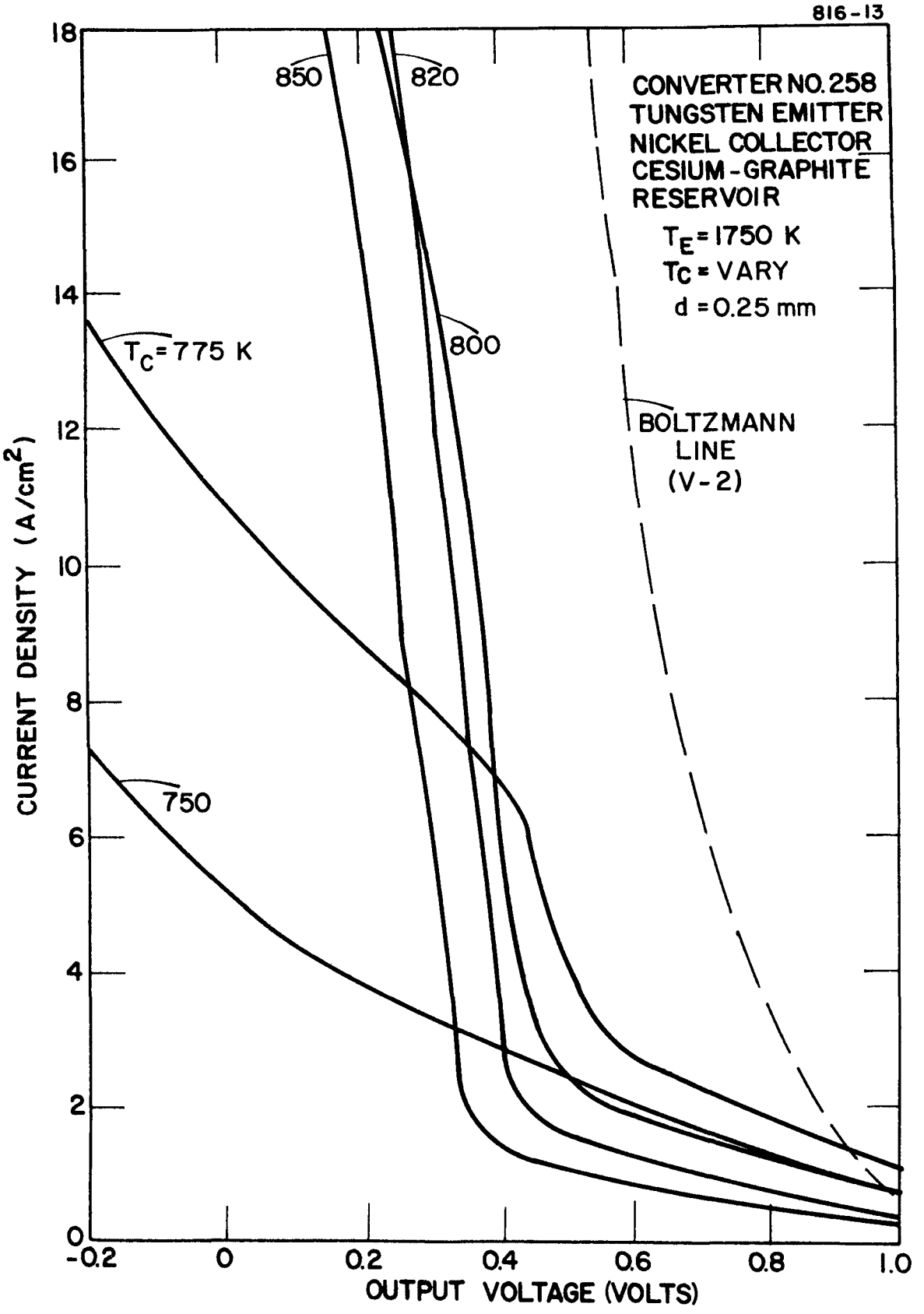

Figure 17. Collector Temperature Family at T_E = 1750 K, d = 0.25 mm in Mode 2 for Converter No. 258

II. COMBUSTION-HEATED CONVERTER DEVELOPMENT

The objective of this task is to develop flame-fired thermionic converters that are as prototypic of projected terrestrial applications as possible. These converters will be constructed with CVD hot shell-emitter structures and designed to minimize expensive materials and construction techniques.

A. Converter No. 239: One-Inch Diameter Hemispherical Silicon Carbide Converter (CVD Tungsten as Deposited Emitter, Nickel Collector)

This converter has been on life test for 6400 hours at an emitter temperature of 1730 K or higher. The performance has been stable during the entire test. At 1750 K, the DC output current is 6.6 A/cm^2 at 0.3 V. The life test will continue.

B. Converter No. 247: Two-Inch Diameter Hemispherical Silicon Carbide Converter (CVD Tungsten as Deposited Emitter, Nickel Collector)

This converter continued on life test at an emitter temperature of 1650 K. The performance and physical appearance of the converter has remained unchanged. At the end of this reporting period, the converter has operated for more than 2000 hours.

C. Converter No. 224: Two-Inch Diameter Torispherical Silicon Carbide Converter

A two-inch diameter torispherical converter (Reference Converter A) was tested during this reporting period. The emitter temperature was 1650 K and the collector and cesium temperatures were optimized. The barrier index for this converter was greater than 2.3 eV. The I-V curves indicated that the electrode spacing was larger greater than optimum.

The diode was taken off test, potted with epoxy and cut in half. The cold spacing was greater than 80 mils instead of 20 mils as in the design. It appears that the ceramic which fixed the spacing did not seat properly during final assembly. A second torispherical converter (Reference Converter A) is being fabricated and will be tested during the next reporting period.

D. Converter No. 263: Two-Inch Diameter Torispherical Silicon Carbide Converter (Liquid Cesium and Cesium-Graphite Reservoir)

A two-inch torispherical converter with a dual cesium and cesium graphite reservoir (Reference Converter B) has been designed. The graphite will be placed in the body of the collector and collector heat exchanger. The converter will have a standard cesium reservoir and the graphite will be charged during the initial operation. Testing should begin during the next reporting period.

E. Four Diode Module Test

The design of this module was described in the last quarterly report. The four CVD silicon carbide diodes are identified as Converter Nos. 250, 251, 252 and 253. Each converter in the four diode module was optimized separately at an emitter temperature of 1600 K. Three diodes showed satisfactory performance while Converter No. 251 performed poorly. Subsequent testing showed that No. 251 had leaked and it was removed from the array. The array was then tested with the three good converters. Figure 18 shows optimized I-V curves for the three-converter module. The "All" curve shows the performance of the three converters connected in electrical series. It is evident from this curve that there are considerable voltage losses from the interconnecting leads. The effect of the lead losses is even more dramatic in Figure 19. Because of this problem, the module has been removed from the furnace and disassembled. New interconnecting leads have been designed and fabricated. Also a replacement diode and a backup diode for Converter No. 251 have been constructed. During the next reporting period, the module will be reinstalled in the furnace and performance tested.

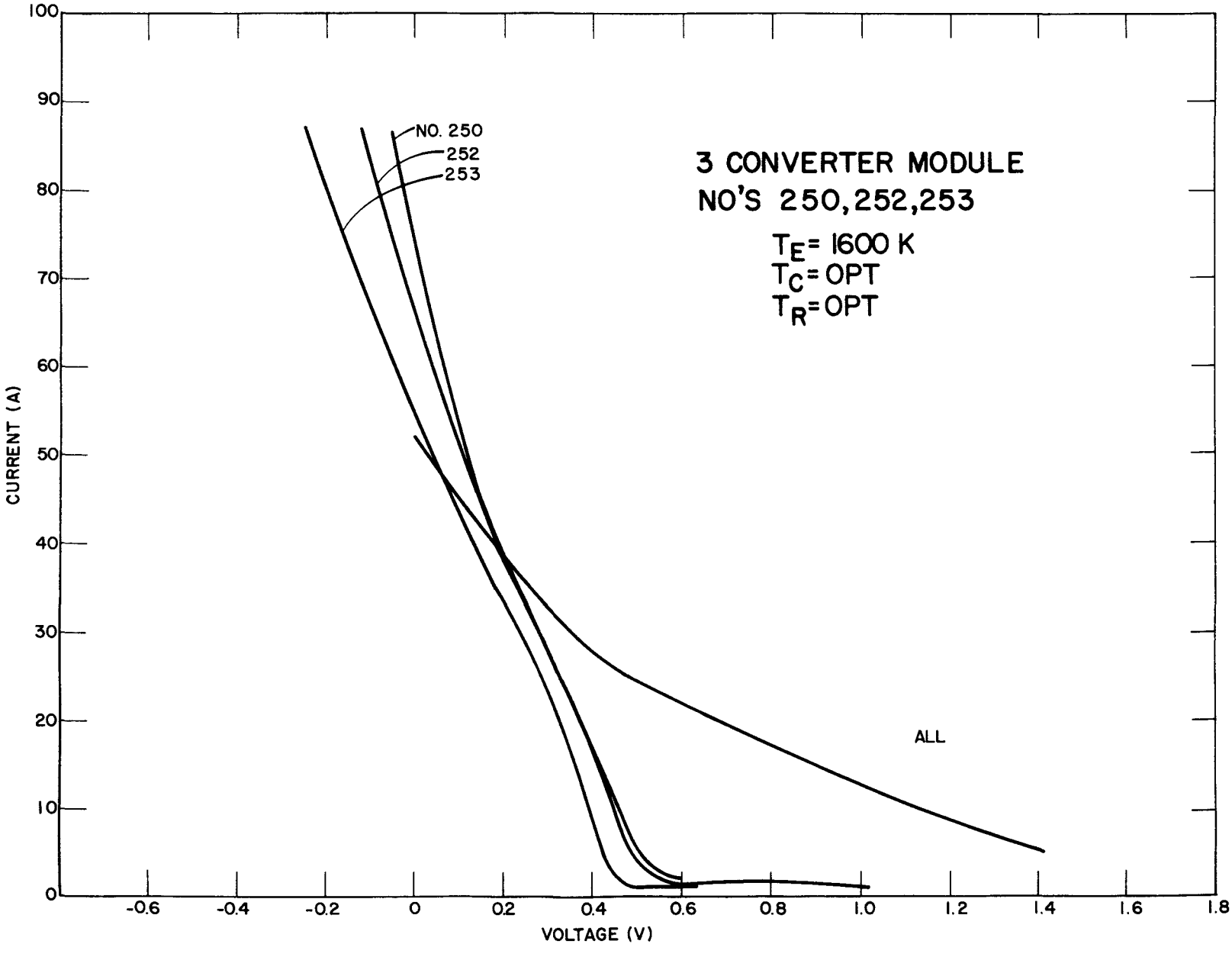

Figure 18. Optimized Performance of Thermionic Module (Three Converters)

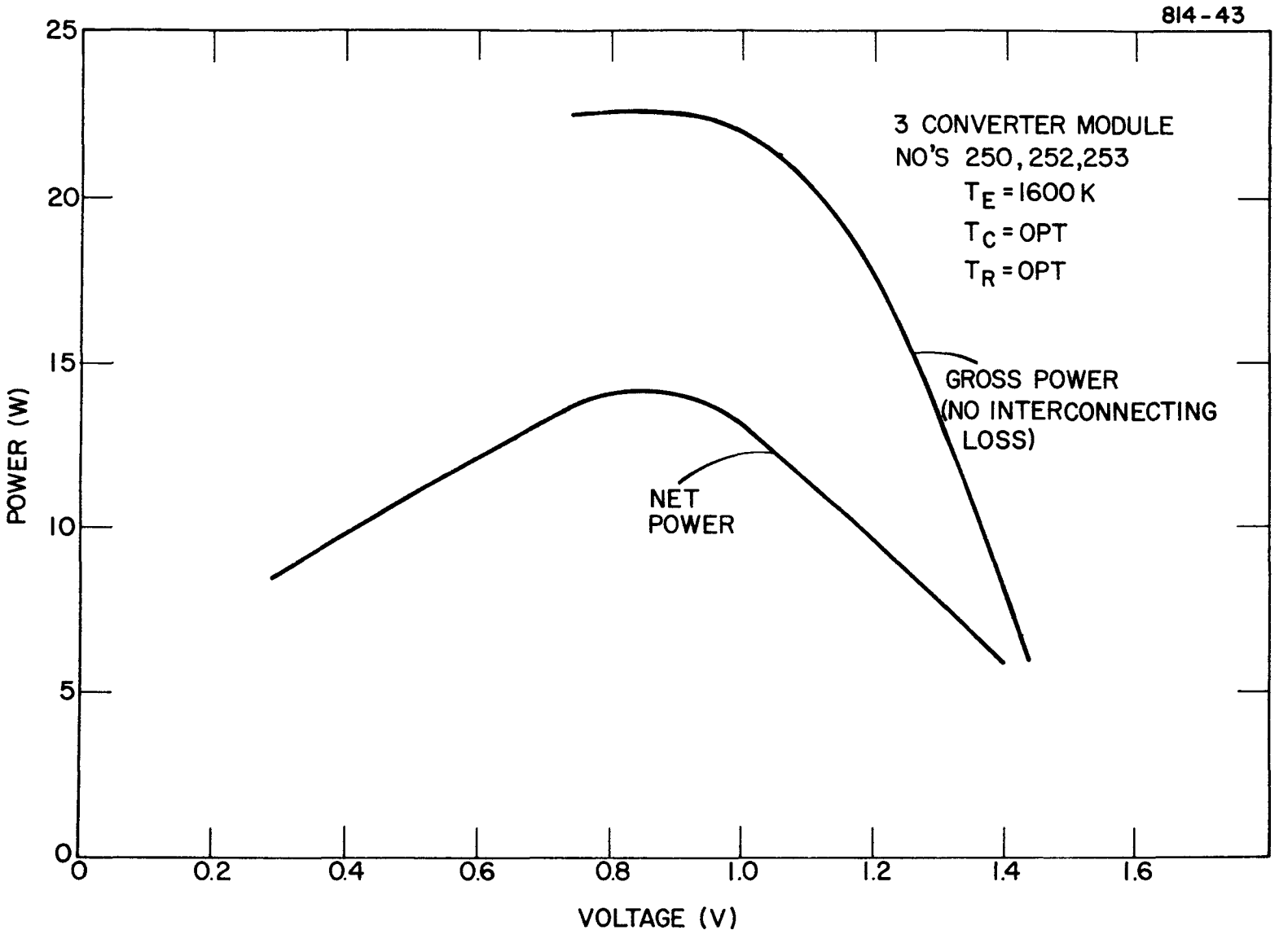

Figure 19. Thermionic Module Power Output with and without Interconnecting Lead Losses

F. Hot Shell-Emitter Flange Life Tests

Testing at operating temperatures continued on the two-inch diameter hot shell-emitter and flange structures. These tests are summarized in Table VII.

During the first part of this reporting period, the multi-converter test furnace was refurbished. New bricks were installed on three of the the walls and additional sight ports were located in the furnace. In addition, three of the recuperators were repaired and one completely replaced.

Shell No. 107 continued to operate at 1600 K without any change. After 2100 hours of operation, it was removed from the furnace and leak checked. No leaks were found and it was again installed in the furnace. At the end of this reporting period, it has operated 2600 hours and the test is continuing.

Shell No. 110 failed after 1092 hours of test at 1600 K. The entire dome of the shell was cracked. The flange area will be sectioned and inspected for oxidation of the copper braze.

TABLE VII

HOT SHELL-EMITTER-FLANGE COMBUSTION TESTS

DESCRIPTION (NUMBER)	NUMBER OF HOURS	TEMPERATURE OF DOME OF SHELL (K)	TEMPERATURE OF FLANGE (K)	TEMPERATURE CYCLES	COMMENTS
1" DIAMETER 4" LONG HEMISPHERICAL HOT SHELL- (101)	110	1925	675 K	9	Black residue on flange. No cracking of structure. Tungsten leaktight.
2" DIAMETER 4" LONG HEMISPHERICAL HOT SHELL (102)	70	1655	675	1	Black residue on flange. SiC cracked and braze swelled.
1" DIAMETER 4" LONG HEMISPHERICAL HOT SHELL (103)	80	1925	850	13	Flange coated with Cermetal 487. SiC cracked at dome. No black residue.
2" DIAMETER 3" LONG HEMISPHERICAL HOT SHELL (104)	2480	1600	850	10	Flange coated with Cermetal 487. SiC leaked 1" from nose. Braze area remained leaktight.
1" DIAMETER 4" LONG HEMISPHERICAL HOT SHELL (105)	70 4 2	1875 1875 2025	675 675 700	20 150 100	Leaktight after 70 hours at 1875 K. Thermal cycles from 900 K to dome temp. Heating and cooling period 30 seconds.
2" DIAMETER 3" LONG HEMISPHERICAL HOT SHELL (107)	2600	1600	850	10	Test continuing
2" DIAMETER 3" LONG HEMISPHERICAL HOT SHELL (108)	230	1600	850	3	SiC cracked one inch from dome.

TABLE VII (Continued)

HOT SHELL-EMITTER-FLANGE COMBUSTION TESTS

DESCRIPTION (NUMBER)	NUMBER OF HOURS	TEMPERATURE OF DOME OF SHELL (K)	TEMPERATURE OF FLANGE (K)	TEMPERATURE CYCLES	COMMENTS
2" DIAMETER 2" LONG TORISPHERICAL HOT SHELL-(109)	1100	1550	850	4	Leak at braze joint.
2" DIAMETER 3" LONG HEMISPHERICAL HOT SHELL (110)	1092	1600	850	4	SiC cracked. Shell destroyed.
2" DIAMETER 3" LONG HEMISPHERICAL HOT SHELL (111)	10	1500	800	1	Test continuing.

III. SYSTEM STUDIES

The objective of this task is to identify and evaluate systems utilizing thermionic energy conversion to improve efficiency and reduce cost. Both powerplant and high-temperature cogeneration processes will be considered.

Stone and Webster Engineering Corporation (SWEC) has prepared a draft of a topical report on the application of thermionic topping to powerplants. This draft was reviewed and returned to SWEC.

A topical report entitled "Topping of A Combined Gas- and Steam-Turbine Powerplant Using a TAM Combustor" (Report No. TE 4258-167-81) has been published and distributed.

IV. CONVERTER PRODUCTION ENGINEERING

The objective of this task is to develop techniques suitable for high-volume production rates which will require automation of assembly and processing steps as well as a modified CVD fabrication method.

Cost analyses have indicated that there would be a significant economic advantage if the graphite mandrel presently used in fabricating hot shell-emitter structures could be replaced by a carbon layer. A comparison of the present fabricating steps for making the hot shell-emitter structure with the projected production quantity procedure is illustrated in Figure 20. Elimination of the graphite mandrel changes the fabrication from a two-step coating process to a three-step coating process. Two methods were evaluated.

In the first method evaluated, silicon carbide would be first deposited on the inside of a graphite mandrel. Next, a layer of carbon would be deposited on the inside of the silicon carbide deposit. Third, a tungsten deposit would coat the inside of the carbon layer. Finally, the trilayer deposit would be separated from the graphite mandrel. After several attempts to implement the first step in this technical approach, it became evident that three problems made this method unworkable. First, a

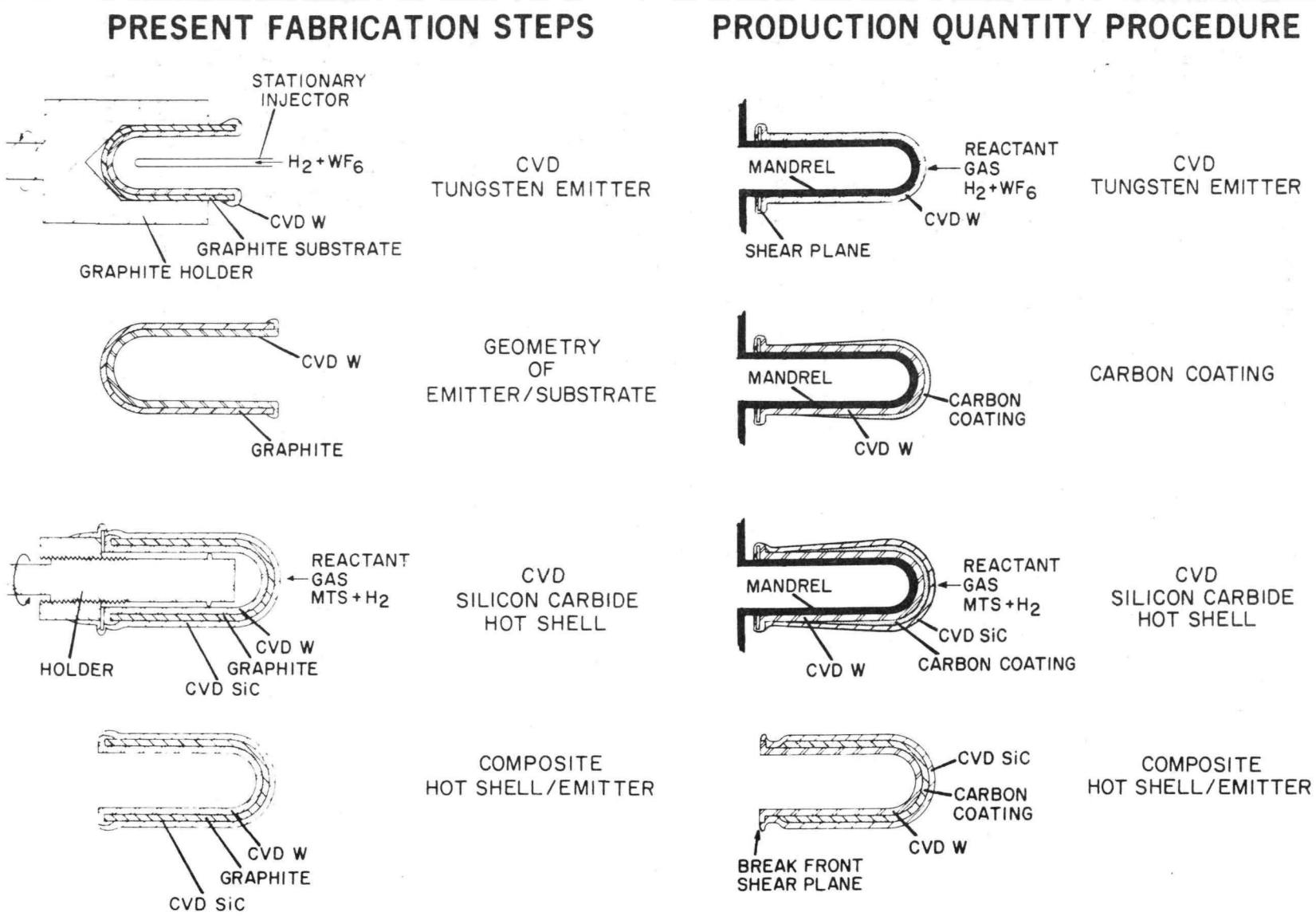

Figure 20. Comparison of Present Fabricating Steps for Making the Hot Shell-Emitter Structure with Production Quantity Procedure

sooty silicon carbide deposit resulted. Second, the deposit was nonuniform with nodules. Third, the silicon carbide could not be removed from the mandrel.

The second method was more successful. First a tungsten layer was deposited on the outside of a graphite mandrel, followed by a layer of carbon, and finally a layer of silicon carbide (see Figure 20).

Initially, a carbon release agent was used to coat the graphite mandrel so that the CVD tungsten could be removed from the graphite after deposition. This carbon release agent was very difficult to remove from the inside of the free-standing tungsten shell. However, experiments demonstrated that if the graphite mandrel is highly polished, the release agent is not required for separation of the tungsten. Some carbon still exists on the inside of the deposit which may affect the thermionic properties of the tungsten. Further work will be required to eliminate carbon residue.

The first carbon mandrels were tapered from a one-inch diameter to a 3/4-inch-diameter spherical dome in order to facilitate the removal of the tungsten deposit.

The present design employs a graphite mandrel with a 3-degree taper which ends with a torispherical dome. The tungsten shell can be removed with no damage to the graphite mandrel. Four 3-inch long tungsten shells were made with the same graphite mandrel. An obvious benefit of this type of deposit is that all tungsten shells have identical inside geometries, making emitter-collector spacing problems easier.

With the outside deposit it is difficult to maintain an even thickness profile of tungsten from the dome to the open end of the shell. There is a tendency for the tungsten deposit at the open end portion of the shell to be quite thin. If a ring shear plane is located about three inches from the dome of the mandrel, the tungsten will break cleanly at that point (as illustrated in Figure 20).

A future step in the development of the production shell will be to locate a molybdenum flange in place of the shear plane (see Figure 21). Tungsten has been successfully deposited onto such a molybdenum flange and removed from the graphite mandrel with the joint between the tungsten and molybdenum remaining leaktight. The tungsten shell and molybdenum flange remained leaktight after cycling in vacuum to 1200 K ten times. If it would be possible to CVD deposit tungsten onto a molybdenum

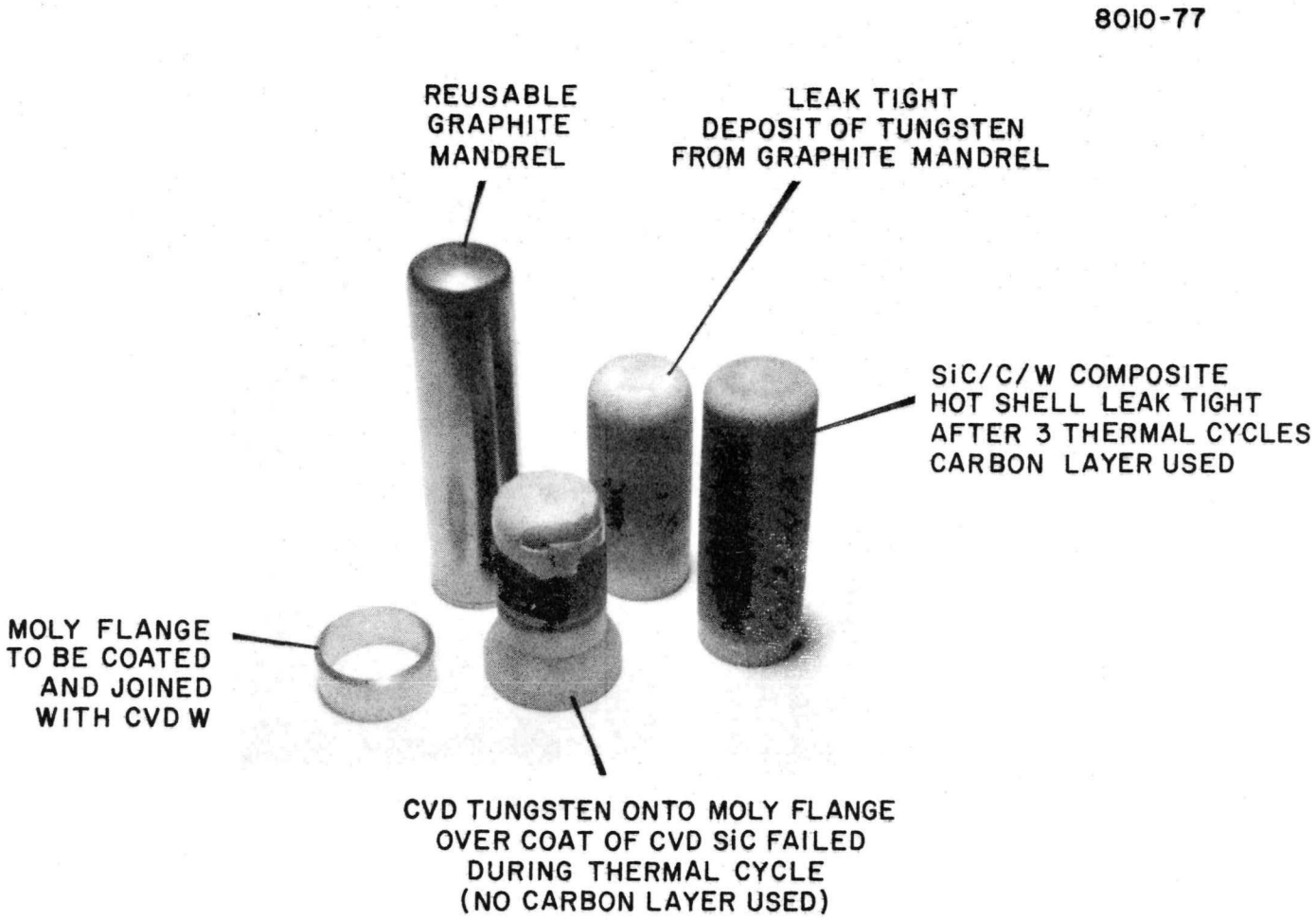

Figure 21. Production Quantity Prototype Hot Shell-Emitter Structures

flange, it would eliminate a copper braze step in the present method of fabrication.

The second step is to deposit carbon onto the tungsten coating. Methane was used in six attempts to coat the tungsten with a carbon. Temperature of the substrate, pressure of the vacuum chamber and concentration of methane were varied. No successful deposit was made on the tungsten shells. Spraying a carbon suspension at room temperature from a conventional spray gun, however, appears encouraging. Thickness and geometry of the carbon coating are easy to vary. A 5-mil coating of carbon was deposited over most of the outside of a tungsten shell. The tungsten near the open end was not coated in order to completely seal the carbon coating with silicon carbide.

Two successful silicon carbide deposits were made on the carbon coating and the tungsten open end. One shell survived thermal cycling in hydrogen to 1400 K.

Three silicon carbide coatings were deposited on tungsten without using an intermediate carbon layer. Although these coatings of silicon carbide appeared to bond well to the tungsten, they cracked when thermally cycled in a hydrogen atmosphere to 1400 K.

REFERENCES

1. DOE/JPL Advanced Thermionic Technology Program Progress Report No. 45, Thermo Electron Report No. TE4258/4247-149-81 p. 11 (1980).

2. M. Bradke and R. Henne, "State of Cermet Electrode Development for Flame Heated Thermionic Converters," Proc. 14th IECEC Conf., p. 1904 (1979).

3. R. Henne, M. Bradke and W. Weber, "Progress in the Development of Small Flame Heated Thermionic Energy Converters," Proc. 15th IECEC Conf. p. 2089 (1980).